Azospirillum brasilense and tomato exudate or cytidine increase phytopathogen resistance and modulate phyllosphere/rhizosphere

Janice N.A. Tagoe[a], Bidya Ojha[a], Shelley M. Horne[a,] and Birgit M. Prüß[a*]

[a]Department of Plant Pathology, Microbiology, and Biotechnology, North Dakota State University, Fargo, ND, 58108

*Corresponding author: Birgit M Prüß (email:Birgit.pruess@ndsu.edu)

Abstract

Tomatoes are an important crop worldwide and phytopathogens can cause devastating losses. Our study describes a treatment, consisting of *Azospirillum brasilense* Sp7 and either tomato seedling exudate or the exudate compound cytidine. The combination of *A. brasilense* Sp7 with cytidine showed a remarkable reduction of 83.4% in disease severity of tomatoes challenged with *Pseudomonas syringae* pv. *tomato* DC3000. Replacing cytidine with exudate was less effective at 71%, but the reduction in disease severity was still larger than by *A. brasilense* Sp7 alone at 55%. This reduction in disease severity was not paralleled by a decrease in *P. syringae* in leaf homogenates. Cytidine caused a 6.7 fold increase in *A. brasilense* Sp7 16S rDNA in root homogenates.

In phyllosphere and rhizosphere, treatments modulated the microbial composition. In the phyllosphere, *A. brasilense* together with cytidine or tomato seedling exudate reduced the presence of eight human and/or plant pathogens in *P. syringae* challenged test groups. In the rhizosphere, principal component analysis revealed that variation along PC1 was dominated by the presence or absence of *A. brasilense*. Intriguingly, the inoculant caused an increase in the abundance of other Azospirillales species.

Les tomates sont une culture d'importance mondiale, et les phytopathogènes peuvent entraîner des pertes dévastatrices. Notre étude décrit un traitement composé *d'Azospirillum brasilense* Sp7 et soit d'un exsudat de plantules de tomate, soit de la cytidine, un composé particulier provenant des exsudats et supposé avoir un effet chimiotactique. L'association de *A. brasilense* Sp7 avec la cytidine a entraîné une réduction remarquable de 83,4 % de la sévérité de la maladie parmi les plantes de tomate infectées par *Pseudomonas syringae* pv. *tomato* DC3000. Le remplacement de la cytidine par des exsudats était moins efficace (71 %), bien que la réduction de la sévérité de la maladie ait demeuré supérieure à celle obtenue avec *A. brasilense* Sp7 seul (55 %). Cette diminution de la sévérité de la maladie n'a toutefois pas été accompagnée d'une réduction de la concentration de *P. syringae* dans les homogénats foliaires. La cytidine a provoqué une augmentation de 6,7 fois de l'ADNr 16S de *A. brasilense* Sp7 dans les homogénats racinaires.

Dans la phyllosphère et la rhizosphère, les traitements ont modulé la composition microbienne. Dans la phyllosphère, *A. brasilense* associé à la cytidine ou aux exsudats de plantules de tomate a réduit la présence de huit agents pathogènes humains et/ou végétaux. Dans la rhizosphère, l'observation la plus remarquable est que la composante (PC1) de l'analyse en composantes principales (ACP) était fortement influencée par la présence ou l'absence de l'inoculum. De manière intéressante, *A. brasilense* Sp7 a entraîné une augmentation de l'abondance d'autres espèces d'Azospirillales.

Keywords: plant growth beneficial rhizobacteria, *Azospirillum brasilense*, cytidine, tomatoes, *Pseudomonas syringae*, phyllosphere, rhizosphere, human and plant pathogens

Introduction

Tomatoes (*Solanum lycopersicum*) are an economically important vegetable crop worldwide (Bergougnoux 2014); losses occur through phytopathogen infections, both fungal (*e.g. Fusarium oxysporum* f. sp. *lycopersici* (Ma et al. 2013)) or bacterial (*e.g. Pseudomonas syringae* pv. *tomato* (El-Fatah et al. 2023)). The latter has been used as a model organism for understanding phytopathogen infection in tomatoes since the 1980s. *P. syringae* pv. *tomato* DC3000 was isolated in 1991 from *Arabidopsis thaliana* (Whalen et al. 1991).

Protection of tomatoes against phytopathogens can be mediated by natural components of the soil microflora designated Plant Growth Promoting Rhizobacteria (PGPR). This includes other species of *Pseudomonas*, such as *Pseudomonas resinovorans*, *Pseudomonas vranovensis*, or *Pseudomonas putida* (Elsharkawy et al. 2023). *Azospirillum brasilense* is currently recognized as a PGPR with ecological function and agricultural biotechnology innovation (Cassán et al. 2026; Cassán 2026). First identified as forming associations with plants in grasslands (Steenhoudt and Vanderleyden 2000), it's uses have extended to monocot crop plants like wheat (*Tritivum aestivum*, (Pereg-Gerk et al. 1998; Vazquez et al. 2021)) or maize (*Zea mays*, (Vidotti et al. 2019)) and dicots including tomatoes (El-Beltagi et al. 2022; Pellegrini et al. 2020). *A. brasilense* colonizes assorted plant tissues, including maize roots (da Cunha et al. 2020) or tomato leaves (Botta et al. 2013). In addition to the nitrogenase system, which is induced under nitrogen limiting conditions (Housh et al. 2023; Wang et al. 2024), benefits from *A. brasilense* colonization for the plants include phytohormone production, changes in root architecture, increased nutrient and water uptake, enhanced leaf development, and increased crop productivity (Cassán et al. 2014; Contreras-Cornejo 2026). Inoculation with *A. brasilense* reshapes the plant microbiome, including a reduction in the abundance of several pathogens (Coniglio et al. 2022).

The rhizospheric lifestyle of *A. brasilense* relies on multiple mechanisms for efficient niche colonization, the first of them being motility and chemotaxis of soil bacteria towards plant exuded metabolites (Nievas et al. 2023). The composition of tomato exudates and chemotaxis towards exudate compounds has been extensively studied (Alexandre 2026; Alexandre et al. 2000; Ganusova et al. 2024; Ganusova et al. 2021; Ganusova et al. 2023). Our own laboratory contributed to this growing body of research by determining the composition of pea, tomato, and cucumber seedling exudate (Nisha et al. 2024). A total of 14 carbon based individual exudate compounds and 9 amino acids were tested for their ability to serve as chemoattractants for *A. brasilense*; the PGPR migrated towards all these compounds on semi-solid swim plates (Nisha et al. 2024). A total of 15 compounds was tested for their ability to enhance root architecture of one week old pea plants (Nisha et al. 2025). The exudate compound cytidine that had tested positive as chemoattractant for *A. brasilense* in the previous study (Nisha et al. 2024) was the only one that increased the number of lateral roots (Nisha et al. 2025).

With this study, we wished to characterize the effect of a combination treatment consisting of *A. brasilense* Sp7 and either tomato seedling exudate or the exudate compound cytidine on phytopathogen resistance of tomatoes, as well as phyllosphere and rhizosphere. In the first part of the study, we tested the hypothesis that tomato seedling exudate or cytidine might enhance the ability of *A. brasilense* Sp7 to aid the tomato plants in resisting infection with *P. syringae* pv. *tomato* DC3000. The effect of the treatments on the abundance of pathogen on leaves and the PGPR on roots was investigated.

In the second part of the study, we looked beyond the tri-partite model of PGPR, phytopathogen, and tomato and investigated the effect of the treatments on phyllosphere and rhizosphere of the tomato plants. A special emphasis was placed on human and plant pathogens.

Materials and Methods

Bacteria and bacterial growth conditions

Bacteria used for this study were *A. brasilense* Sp7 (Eskew 1977), kindly provided by Dr. Gladys Alexandre (University of Tennessee, Knoxville, TN) and *P. syringae* pv. *tomato* DC3000 (ATCC BAA-871) (Buell et al. 2003). *A. brasilense* Sp7 was cultured in Tryptone Yeast extract (TY: tryptone, 5 g/l; yeast extract, 3 g/l; $CaCl_2 \cdot 6H_2O$, 1.3 g/l (Beringer 1974)). *P. syringae* pv. *tomato* DC3000 was grown in liquid King's B medium (20 g/l proteose peptone, 1.5 g/l K_2HPO_4, 10 ml/l glycerol, 1.5 g/l $MgSO_4 \cdot 7\ H_2O$), pH 7,2 $\pm$ 0.2) (King et al. 1954), supplemented with 50 µg/ml rifampicin. For agar plates, 15 g/l agar were added.

Tomato seeds and seed germination

Yellow pear tomato seeds (SKU34924) were from True Leaf Market (Salt Lake City, UT). Seeds were surface-sterilized for 30 s in 95% ethanol and 5 min in 2% bleach, then rinsed 10 times with sterile dH_2O (dH_2O). Seeds germinated for 3 days on 0.8% agar in dH_2O. For experiments with seedling exudate, tomato exudate was produced from 1 g of freshly germinated seeds in 10 ml of dH_2O (Nisha et al. 2024). Seeds germinated under three separate conditions: dH_2O, seedling exudate at 1.5 mg of exudate dry weight/ml dH_2O, or cytidine at 100 mM. Germinated seeds were planted when approximately half an inch of root was visible.

Plant growth

To permit maximum colonization with our inoculant in the initial days of plant growth (Bashan and De-Bashan 2002; King et al. 2024; Querejeta 2023), we sterilized the growth medium by autoclaving. The medium was a 1:1 (w/w) mix of soil (Promix BX General Purpose, 10280; Premier Horticulture Inc. Canada, Québec, Canada) and vermiculite (Vermiculite Medium PVP; PVP Industries, North Bloomfield, OH). Germinated seeds were planted into the

center of pots of ~4 inch in diameter and 6 inch in height. *A. brasilense* Sp7 was inoculated immediately to the location of the planted seed at 10^3 to 10^4 CFU in 1 ml of dH_2O. Plants were grown in a Gen 2000 growth chamber (Conviron, Pembina, ND) at 26°C and light for 16 hours. We used Tomato-tone (The Espoma Company, Millville, NJ) as fertilizer following the manufacturer's instructions.

Phytopathogen experiment and disease assessment

Tomato seedlings germinated in dH_2O, exudate, or cytidine were planted and inoculated with/without *A. brasilense* Sp7. Four weeks old tomato plants were dip-inoculated with *P. syringae* pv. *tomato* DC3000 as previously described (Chakravarthy et al. 2017). Briefly, plants were dipped for 30 s in 3 x 10^7 CFU ml^{-1} in 10 mM $MgCl_2$, then air dried and incubated in a Gen 2000 growth chamber at 26°C with 80% relative humidity and 16 h of light. Control groups of un-challenged plants were dipped in $MgCl_2$ as part of the first experiment and compared to un-dipped plants. Neither of these plants exhibited disease symptoms and live counts were similar. For this reason, un-challenged control groups in the consecutive experiments were no longer dipped. Six days after the challenge, plants were photographed and assessed for disease severity.

Disease severity data were collected from three replicate experiments in twelve test groups. Symptoms started with dark necrotic lesions on leaves, then leaf wilting. In severe cases, this was followed by leaf and ultimately plant death. We expressed disease severity as percent death of the leaves from each plant. One healthy plant that had not been challenged with the pathogen and one severely diseased plant were used as comparisons. The assessment was done by at least two researchers in steps of 10%. Examples of plants that were assessed as 0% dead, 50% dead, and 90% dead are presented in Figure S1.

For *Pseudomonas* counts, we collected data from two replicate phytopathogen experiments. Live bacterial counts were obtained from homogenates that were produced from 6 leaf discs per plant that were punched with a 1/4 inch sterile cork borer. Weighed leaf discs were homogenized in 10 mM $MgCl_2$ with pestles. The leaf homogenates were serially diluted and plated onto King's B agar to determine *Pseudomonas* counts (King et al. 1954). Bacterial counts were expressed as $\log_{10}$ CFU/g of plant material.

For disease severity and *Pseudomonas* counts, data were presented as Box and Whiskers generated with GraphPad Prism 10.6.1 (892). The lines within the boxes indicate the medians of the populations. Data points from individual plants are included, means of the populations are given for pathogen challenged test groups. Statistical analysis was done by one-way ANOVA, followed with Tukey for pairwise comparisons between test groups. A *p*-value below 0.05 was indicative of a statistically significant difference between test groups. Percent disease reduction was calculated as $\left\{\mathbf{100} - \left\{\frac{\mathbf{c}}{\mathbf{t}}\right\}\right\}$, where t are the mean percent death data from the treatment groups and c the mean percent death data from the untreated control group (-*Abra* +Ps).

16S rDNA analysis

For the determination of bacterial communities, gDNA was isolated from leaf and root homogenates from three plants from one phytopathogen experiment. Prior to homogenizing the roots, we washed them with dH_2O thoroughly but carefully, so that most of the soil would be gone, but the outside of the roots would still be intact. This sampling would give us the epiphytic and endophytic microbiomes of the roots.

Homogenates were produced from approximately 50 mg of plant material by using the Cole-Parmer HG-200 GenoLyteR Compact Homogenizer (Cole-Parmer, Vernon Hills, IL) at 2,000 rpm for 1 min. DNA extraction was done with the Qiagen Plant Pro kit (Qiagen, Hilden,

Germany). Quality of the DNA samples was analyzed with the Nanodrop One Spectrophotometer, quantity with the Qubit 4 Fluorometer (Fisher Scientific, Hampton, NH). Samples were diluted to 1 ng/µl. The construction of the library and 16S rDNA sequencing were done at the Dr. Thomas Glass Biotech Innovation Core at NDSU. We used the QIAseq 16S/ITS Region Panel (Qiagen) for the generation of the 16S rDNA library. The primers used were 341f:CCTACGGGNGGCWGCAG and 785r:GACTACHVGGGTATCTAATCC, which amplify the V3/V4 hyper variable region of the 16S rDNA (Qiagen). We followed the PCR protocol from the manufacturer and cleaned the resulting PCR products with QIAseq bead cleanup. The index PCR reaction was done with unique dual indexes for each sample, PCR products were cleaned with QIAseq bead cleanup. Samples were quantified with the Qubit 4 Fluorometer and analyzed with the 4200 Tape Station (Agilent, Santa Clara, CA). Sequencing was performed using the P1 XLEAP-SBS 600 cycle sequencing kit on the NextSeq 1000 (Illumina, San Diego, CA).

Phyllosphere and rhizosphere data were analyzed separately. Fastq files were imported into CLC Genomics Workbench (Qiagen) for analysis using the Microbial Genomics Module. The Data QC and OTV clustering workflow was used to trim adaptors, poly G regions, ambiguities and sequences not meeting the quality threshold of 0.05. Reference based OTV clustering using the Silva SSU 99% (138.2) database was performed using the similarity percent specified by the database. Minimum occurrence was set at 2. The species identifiers or taxonomies in the CLC Workbench are from the Earth Microbiome Project (https://earthmicrobiome.org/). The resulting abundance tables were exported to Excel separately for phyllosphere and rhizosphere and further analyzed. These two tables are provided as online supplements and include the ASV (Tables S1 and S2). Rarefaction curves for both data sets are shown in Figure S2.

Step 1 of the analysis was to identify our inoculant *A. brasilense* Sp7 and our challenge *P. syringae* pv. *tomato* DC3000 among the bacterial species that the CLC Workbench bioinformatics analysis associated with the ASVs according to the Earth Microbiome Project. We grew liquid cultures of each strain and included the data in separate columns of Table S2; our inoculant *A. brasilense* Sp7 was *A. brasilense* AF533354.1.1439 in column BG and our challenge *P. syringae* pv. *tomato* DC3000 was *P. amygdali* pv. *morsprunorum* AB0011445.1.1538 in column BH. For additional confirmation, ASV from *P. amygdali* was subjected to BLAST analysis (https://blast.ncbi.nlm.nih.gov/Blast.cgi). These data are included in Table S3 and serve as additional confirmation that *P. amygdali* pv. *morsprunorum* is indeed our phytopathogen *P. syringae* pv. *tomato* DC3000.

Step 2 was to filter out small abundances that added a lot of taxonomies to the data set but not a lot of information. In the less complex data set of Table S1, we filtered out DNA abundances (rows) from taxonomies that had combined abundances $\leq$49, added across all test groups and replicates (36 columns). In the more complex data set of Table S2, we filtered out abundances from taxonomies that had combined abundances $\leq$499. We removed plant and fungal taxonomies.

Step 3 was the analysis of 16S rDNA abundances from our challenge pathogen *P. syringae* pv. *tomato* DC3000 in the phyllosphere and our inoculant *A. brasilense* Sp7 in the rhizosphere. In Table S1, we used the data on the *P. syringae* DC3000 tab. In Table S2, we used the data on the *A. bra* tab. The data sets were statistically analyzed with one-way ANOVA to compare either all 12 test groups or just the six pathogen challenged test groups (+Ps). Data were presented as floating bars in GraphPad Prism.

Step 4 was the generation of a phylogenetic tree for the phyllosphere. We used the 67 taxonomies from Table S1 in the >50 tab. ASV were converted into a FASTA file and loaded into Galaxy (usegalaxy.eu/). We performed a multiple sequence alignment with MAFFT, followed by FASTTREE. The Newick file (.nhx) from the maximum likelihood computation was used in iTOL (itol.embl.de). Using the mid-point root, the circular tree was selected. Note that the taxonomies were abbreviated as part of the production of the FASTA file. Abbreviations are included in Table S1 as a separate column (B) on the >50 tab.

Step 5 was the analysis of 16S rDNA abundances within phyllosphere and rhizosphere. First, we computed richness, separately for each replicate in Excel with the following function: =countif(A2:A69, “>1”). Second, relative abundances were summed over the 67 taxonomies from the phyllosphere and the 280 taxonomies from the rhizosphere, also separately for each of the three replicates in Excel. For both analyses, data were transferred into GraphPad Prism and graphed as floating bars. Third, for the generation of the heatmaps, 16S rDNA abundances from taxonomies that represent the different bacterial orders were summed across all species. Mean percent abundances across the three replicates were used and visualized in GraphPad Prism. For the phyllosphere, only pathogen challenged test groups were included in the heatmap. Fourth, the same data set was used for principal component analysis (PCA) in GraphPad Prism, graphing PC scores (treatments) and Biplot analysis (treatment and orders). We computed association strength between treatments and orders with cosinus similarity.

Step 6 was the analysis of human and plant pathogens at species level in the phyllosphere, focusing on the three bacterial orders with the largest abundances, Enterobacterales, Pseudomonadales, and Xanthomonadales. Focusing on the most abundant pathogens, we selected taxonomies that had a sum abundance across all test groups and

replicates ≥ 1,000. For the resulting eight human and/or plant pathogens, we generated a heat map in Graph Pad Prism.

Digital PCR

From the same DNA samples that were used for 16S rDNA sequencing, we performed digital PCR to confirm 16S rDNA data for our challenge pathogen *P. syringae* pv. *tomato* DC3000. Primers for *P. syringae* pv. *tomato* DC3000 were PST-*hrpL*_e_fwd, 5'-TTTCAACATGCCAGCAAACC-3' and PST-*hrpL*_e_rev, 5'-GATGCCCCTCTACCTGATGA-3' as described (Peňázová et al. 2020). The probe was PST-*hrpL*_TP, 5'-GCTGAACCTGATCCGCAATCAC-3', marked with the yellow fluorescence dye HEX.

Each PCR reaction mix of 40 µl contained between 50 and 200 ng of DNA, 1 x PCR mix, 0.8 µM primer mix, 0.4 µM probe, and 0.25 U EcoRI in RNAse free water. The PCR reactions were performed in a QIAcuity Digital PCR System (Qiagen) on 24 well QIAcuity Nanoplates at 40 cycles of annealing/extension at 55°C for 30 s and denaturation at 95°C for 15 s. After 40 cycles, fluorescence was measured in each of the 25,000 partitions of a well. Individual reactions were considered positive when a threshold of 50 to 150 was achieved. The original data were expressed as count of positive and negative reactions in the partitions and computed to copies/µl in the QIAcuity Software Suite v2.1.7.182. Given the start concentration of DNA, these data were converted to copies/ng of DNA. Data were graphed as floating bars in GraphPad Prism, statistical analysis was done with ANOVA.

Results

Treatments decreased disease severity on pathogen challenged tomatoes

The first goal of our study was to investigate the effect of the treatments on phytopathogen resistance of the tomatoes. The experiment was done in 12 test groups, covering

absence or presence of each of the following: *A. brasilense* Sp7 (*Abra*), *P. syringae* pv. *tomato* DC3000 (Ps), seedling exudate (Ex), or cytidine (CYD). Fig. 1 shows disease severity data expressed in percent death at 6 days post challenge.

The *p*-value from the one-way ANOVA across the 12 test groups was <0.0001. These were also the *p*-values from the Tukey pairwise comparisons for the six comparisons between plants challenged or not challenged with *P. syringae* pv. *tomato* DC3000 (*p*-values not included in Fig. 1). In the absence of the pathogen, disease severity ranged between 1% and 2% death (white bars). For the three comparisons between *P. syringae* challenged plants that were either inoculated or not inoculated with *A. brasilense* Sp7 (-*Abra* +Ps versus +*Abra* +Ps; -*Abra* +Ex +Ps versus +*Abra* +Ex +Ps; -*Abra* +CYD +Ps versus +*Abra* +CYD +Ps) (*p*-values in purple), the *p*-values indicated statistical significance of the differences. *A. brasilense* Sp7 had a positive effect on the health of the challenged plants. The -*Abra* +Ps vs +*Abra* +Ps comparison yielded a disease reduction of 55% from 80.3% to 36.1% leaf death.

An improvement in disease reduction by *A. brasilense* Sp7 was accomplished by germinating seeds in seedling exudate (*p*-values in red) and more so in cytidine (*p*-values in green). Comparing the test group -*Abra* +Ps at 80.3% death to +*Abra* +Ex +Ps at 23.3% death, the reduction in disease severity was 71% at a *p*-value indicating statistical significance of the difference. Comparing the test group -*Abra* +Ps at 80.3% death to the test group +*Abra* +Cyd +Ps at 13.3% death, the reduction in disease severity was 83.4% at a *p*-value below 0.05.

The treatments did not decrease abundance of the pathogen on leaves, cytidine increased abundance of the PGPR on roots

The reduction in disease severity by the treatments could have multiple causes; among the possibilities are a decrease in the abundance of *P. syringae* on leaves or an increase in the abundance of *A. brasilense* on roots.

The abundance of *P. syringae* was determined as *Pseudomonas* counts on King's B medium, abundance of 16S rDNA by means of sequencing, and copies of the *hrpL* gene by means of digital PCR. Note that King's B medium detects multiple microorganisms in addition to species from the *Pseudomonas* genus, in particular those that produce fluorescent siderophores (Johnsen and Nielsen 1999), the *hrpL* gene is specific for *P. syringae* (Peňázová et al. 2020), and 16S rDNA is specific for our *P. syringae* pv. *tomato* DC3000.

Fig. 2A shows the $\log_{10}$ CFU/g data from the colony counts. Pathogen challenged plants contained a mean of 8.1 to 9.25 $\log_{10}$ CFU of *Pseudomonas*/g of plant material (red bars). Un-challenged plants contained a smaller but still remarkable number of *Pseudomonas* and/or other fluorescent bacteria between 4.2 and 7.25 $\log_{10}$ CFU/g (white bars). The only statistically significant differences from the pairwise comparisons were five out of six comparisons where a test group of plants challenged with *P. syringae* pv. *tomato* DC3000 was compared to an un-challenged group (*e.g.* -*Abra* +Ps versus -*Abra* -Ps). A second ANOVA was performed to compare the six test groups of challenged plants. The *p*-value for this comparison did not indicate statistically significant differences between challenged test groups.

Fig. 2B shows data from the 16S rDNA analysis. The *p*-value from the one-way ANOVA that was performed across all twelve test groups indicated statistically significant differences between test groups. However, calculating an ANOVA across only the six un-challenged test groups was 0.1740. The only statistically significant differences were between test groups whose

sole treatment difference was presence or absence of the pathogen. Leaf homogenates from un-challenged tomato plants did not contain 16S rDNA from the challenge pathogen.

Fig. 2C shows copies of the *hrpL* gene larger than 1/ng of DNA only for test groups that had been challenged with the pathogen (red bars). The ANOVA that was computed across all 12 test groups did point towards statistically significant differences with a *p*-value of 0.0082. The ANOVA across the six pathogen challenged test groups was 0.1157. In three experiments, our treatments did not reduce the abundance of *P. syringae.*

For the abundance of *A. brasilense* on roots, we performed the same types of experiments as for the abundance of *P. syringae* from root homogenates, live counts from TY strep plates, 16S rDNA, and dPCR (Reddy Priya et al. 2016). Fig. 3 shows the 16S rDNA analysis for *A. brasilense* Sp7. The ANOVA that was performed on the complete data set yielded a *p*-value of statistical significance. When comparing the +*Abra* -Ps test group with the +*Abra* +CYD -Ps group, cytidine increased 16S rDNA abundance for *A. brasilense* Sp7 by 6.7 fold with *p*-values of 0.0004 and 0.05 from the parametric *t*-test and the non-parametric Mann-Whitney U test, respectively. We did not obtain live counts from the TY strep plates or PCR products from the dPCR. We observe that cytidine increased the abundance of *A. brasilense* Sp7 on tomato roots.

Treatments modulated the phyllosphere of phytopathogen challenged tomatoes

The second goal of this study was to determine the effect of the treatments on the tomato microbiome. The first analysis was designed to get a glance at the microbial diversity included in our tomato microbiome across all treatment groups to permit comparison with published data (Dong et al. 2019; Romero et al. 2014).

The phyllosphere (Table S1) initially contained 685 taxonomies, which we narrowed down to 67, applying the >50 filter. Fig. 4 shows the phylogenetic tree including these 67

taxonomies that were represented in any of the 12 test groups. The taxonomies clustered into two phyla, Proteobacteria and Bacteroidota. There are 5 species of Sphingomonadales (purple) and 5 species of Rhizobiales (green) among the Alphaproteobacteria, 3 species of Burkholderiales (brown) from the Betaproteobacteria, as well as 2 species of Xanthomonadales (dark purple), 24 species of Pseudomonadales (blue), and 28 species of Enterobacteria (orange) among the Gammaproteobacteria. The order Enterobacterales included the families of *Erwiniaceae* and *Enterobacteriaceae*, the Pseudomonadales were all from the family *Pseudomonadaceae* and the genus *Pseudomonas*. The two species of Bacteroidota were *Flavobacterium ginsengiterrae* from the order Flavobacteriales (yellow) and *Pedobacter kyungeensis* from the order Sphingobacteriales (red). Overall, our leaf homogenates included predominantly species from the Proteobacteria.

The following analyses were targeted towards understanding the effect of the treatments on microbial composition. Richness (Fig. 5A) and sum abundances (Fig. 5B) were computed separately for each of the 3 replicates/test groups from the 67 phyllosphere taxonomies. Both analyses pointed towards an almost complete lack of 16S rDNA within the phyllosphere of tomatoes that had not been challenged with *P. syringae* pv. *tomato* DC3000. Plants from the test groups -*Abra* +Ex -Ps and -*Abr*a +CYD -Ps harbored a small number of species (Fig. 5A). For richness (Fig. 5A), five out of six comparisons between test groups whose only treatment difference was challenge or no challenge with the pathogen had a *p*-value below 0.05. For sum abundances (Fig. 5B), the *p*-value from the one-way ANOVA indicated that differences between test groups were lacking statistical significance. By all appearances, the presence of the pathogen permits rise to a myriad of bacteria. Among the pathogen challenged test groups, +*Abra* +Ex +Ps

exhibited low richness and low sum abundance. The test groups -*Abra* + Ps and +*Abra* +CYD +Ps had low sum abundances (Fig. 5B).

Fig. 5C visualizes the percentage of 16S rDNA abundances that were summed across all taxonomies from each of the 8 orders and expressed as percent. Enterobacterales, Pseudomonadales, and Xanthomonadales were the only ones that had significant relative abundances. The highest abundance for Enterobacterales was seen in the +*Abra* +Ex +Ps test group at 68%. There was a reduction in the abundance of 16S rDNA in the +*Abra* +CYD +Ps test group at 9.8% relative to the -*Abra* +CYD +Ps group at 17.4%. For Pseudomonadales, there was a reduction in abundance in the +*Abra* +Ex +Ps test group at 27% relative to the -*Abra* +Ex +Ps group at 75%. For Xanthomonadales, there was a reduction in abundance in all three +*Abra* test groups relative to the respective -*Abra* group.

To investigate associations between test groups and abundances of bacterial orders, we performed PCA, using the mean of the percent abundances (Figs. 5D and E). PC1 captured 66% of the total variation and PC2 captured an additional 25.09% to a cumulative coverage of 91.08%. The six treatments grouped distinctly within the PC space, implying strong multivariate separation between treatments (Fig. 5D). The furthest outlier appeared to be the +*Abra* +Ex +Ps group (yellow) with the PC1 coordinate 2.71 and the PC2 coordinate -2.091. Enterobacterales associated strongly with this +*Abra* +Ex +Ps test group (yellow) in the biplot (Fig. 5E) with a cosinus similarity of 0.924. Pseudomonadales associated with the +*Abra* +CYD +Ps group with a cosinus similarity of 0.998 and with the -*Abra* +CYD +PS group with a cosinus similarity of 0.836 (both light blue in Fig. 5D and E). Across the five analyses that are covered with Fig. 5, the +*Abra* +Ex +Ps and +*Abra* +CYD +Ps test groups stood out, indicating that the respective treatments modulate the phyllosphere.

At the species level, we were interested in the effect of the treatments on human and/or plant pathogens and generated a heat map from the potential pathogens that are included in the Enterobacterales, Pseudomonadales, and Xanthomonadales with a sum abundance >1,000 across all test groups (Fig. 6). There is the general observation that the +*Abra* +Ex +Ps and +*Abra* +CYD +Ps groups were low in abundances for all tested pathogens. Abundances of 16S rDNA for *Pantoea ananatis* and *Pseudomonas fulva* were low across all test groups. It seems like our treatments may not reduce the abundance of our challenge pathogen, but they do reduce abundance of other pathogens. For evidence of a bacterial species being a human or plant pathogen, see Table S4.

Treatments modulated the rhizosphere of phytopathogen challenged tomatoes

In similarity to the phyllosphere, our first rhizosphere analysis was designed to get a glance of the microbial diversity included in our tomato microbiome across all treatment groups to permit comparison with published data. We initially obtained 8,619 taxonomies, which we narrowed down to 280, applying the much more restrictive >500 filter (Table S2). Among the proteobacteria, there were 93 species of Alphaproteobacteria, 42 species of Betaproteobacteria, and 43 species of Gammaproteobacteria. The non-proteobacteria clustered into eight phyla; Bacteroidota with 61 species, Actinobacteriota with 16 species, Bdellovibrionata with 10 species, Planctomycetota with 4 species, Patescibacteria with 3 species, Myxococcota with 2 species, and Abditibacteriota and Acidobacteria with 1 species each.

To determine the effects of the treatments on microbial composition, richness (Fig. 7A) and 16S rDNA abundances (Fig. 7B) were computed from all 280 taxonomies within the rhizosphere. Both, richness (Fig. 7A) and sum abundances (Fig. 7B) showed 16S rDNA within

the rhizosphere of all twelve test groups of plants. For both analyses, the *p*-value from the one-way ANOVAs pointed towards a lack of statistical significance of any differences.

Fig. 7C shows the heatmap for the 29 bacterial orders in percentage of 16S rDNA abundances. One highly abundant order were the Rhizobiales, especially in the -*Abra* -Ps group at 30.85%, in the +*Abra* -Ps group at 28.59%, the -*Abra* +Ex +Ps group at 27.27%, the -*Abra* +Ex -Ps group at 25.52%, and the -*Abra* +CYD -PS group at 24.5%. Pseudomonadales were high (>24%) in the -*Abra* +Ps, -*Abra* +Ex +Ps, -*Abra* +CYD +Ps and -*Abra* +CYD -Ps groups and lower in the +*Abra* groups. Burkholderiales had the highest percent abundance among any bacterial orders in the +*Abra* +Ps group at 32.9%. In the +*Abra* +Ex +Ps group, Burkholderiales were still high at 28.46%. Flavobacteriales were high in the -*Abra* -Ps group at 23.55%, the -*Abra* +Ex +Ps group at 25.05%, and the -*Abra* +CYD +Ps group at 24.15%. Bacteriovoracales were high in the -*Abra* +Ex –Ps group at 21.04%.

Fig. 8 shows the results from the PCA analysis that was computed from the mean of the percent abundances. In Figs. 8A and 8B, PC1 captured 35.65% of the total variation and PC2 captured an additional 15.05% to a cumulative coverage of 50.7%. Treatments with "+A" resembling the presence of *A. brasilense* Sp7 were located on the positive side of the y-axis, while treatments designated "-A" resembling the absence of the inoculant clustered on the negative side (Fig. 8A). This suggests that PC1 was strongly influenced by presence or absence of the PGPR. From the PCA, we calculated association strengths as cosinus similarity. Micrococcales, Azospirillales, Salinisphaerales, and Microtrichales associated positively with the presence of *A. brasilense* Sp7 (Table S5). Flavobacteriales, Pseudomonadales, Propionibacteriales, Saccharomonadales, Rhizobiales, Tepidisphaerales, and Abditibacterales associated positively with the absence of *A. brasilense* Sp7 (Table S5).

Discussion

Our combination treatments of *A. brasilense* Sp7 and tomato seedling exudate or cytidine reduced disease severity of tomatoes after challenge with *P. syringae* pv. *tomato* DC3000. This effect was larger for the treatment that included cytidine than the one including total exudate. The reduction in disease severity was not paralleled by a decrease in the abundance of *P. syringae* on leaves, but by an increase in *A. brasilense* Sp7 on roots by cytidine. The treatments modulated the relative abundances of several bacterial orders within phyllosphere and rhizosphere, including several species of human or plant pathogens in the phyllosphere and species from the order Azospirillales in the rhizosphere.

Phytopathogen resistance

P. syringae pv. *tomato* DC3000 has been used to model infectious disease in plants (Chakravarthy et al. 2017; Janda et al. 2023; Lindeberg et al. 2009; Namgung et al. 2019; Wei and Collmer 2018; Xin and He 2013), the initial colonization is helped by chemotaxis and motility towards plant exudates (Cerna-Vargas et al. 2019; Elsharkawy et al. 2023; Santamaría-Hernando et al. 2022). The backbone of our phytopathogen experiments are the studies by the laboratories of Dr. Emilia Lopez-Solanilla (Cerna-Vargas et al. 2019), Dr. Melanie Filiatrault (Chakravarthy et al. 2017), and Drs. Yoav Bashan and Luz de-Bashan (Bashan and De-Bashan 2002); the original protocols were modified by the supplementation with cytidine or total seedling exudate in the germination step and *A. brasilense* Sp7 at planting.

The general observation that our treatments suppressed disease severity is consistent with many previous studies on disease suppression by PGPR and exudate compounds. Tomatoes are capable of exuding a wide array of metabolic intermediates into the soil to promote their own health and disease resistance. Examples include methyl ferulate preventing tobacco black shank

disease (Ma et al. 2025), benzoxazinoids that stimulate chemotaxis (Baatsen et al. 2025), oxylipins that prevent foliar phytopathogens (Huang et al. 2023), glycoalkaloids to modulate microbial communities and defend against pathogens (Nakayasu et al. 2022; Nakayasu et al. 2021), and acyl sugars acting as insecticides (Korenblum et al. 2020). Improving resistance towards diseases and environmental stressors has been accomplished by applying exudate compounds to the soil (Dong et al. 2019; Wen et al. 2023). A recent review article summarized exudates as a bridge between roots and rhizospheric microbes (Feng et al. 2024).

The disease reduction in this study is impressive at 83.4% (Fig. 1). Possible causes for this high reduction are numerous. One obvious cause could be a decrease in the abundance of pathogen on the leaves, as was seen for inoculation of tomatoes with *A. brasilense* but without seedling exudate or cytidine (Bashan and De-Bashan 2002). In three different experiments, we came to the conclusion that abundance of the pathogen was not decreased (Fig. 2). It is noteworthy that live *Pseudomonas* counts were still high in plants that had not been challenged with the pathogen at 4.2 to 7.2 $\log_{10}$ CFU/g. This is because King's B medium does not just detect *P. syringae*, but other species from the genus *Pseudomonas* and other microorganisms that produce fluorescent siderophores (Johnsen and Nielsen 1999). The 16S rDNA analysis and dPCR (Peňázová et al. 2020) were more selective for *P. syringae* and led to the conclusion that there was little or no *P. syringae* on leaves of plants not challenged with the pathogen.

A second possible cause for disease suppression might be an enhancement of colonization by our inoculant *A. brasilense* Sp7 in response to seedling exudate or cytidine. The phyllosphere did not contain any detectable abundances of *A. brasilense* Sp7 16S rDNA, but cytidine increased *A. brasilense* Sp7 16S rDNA in the rhizosphere by 6.7 fold (Fig. 3). This increase was only seen in the 16S rDNA experiment, as live bacterial counts and dPCR failed to

detect signals for *A. brasilense* Sp7. We believe this is due to low abundances of *A. brasilense*, a problem that has been observed before (Compant et al. 2025).

An increase in colonization by the PGPR might lead to an increase in the induced systemic response of the tomatoes, a state of enhanced defensive capacity of the plants after colonized by certain PGPR. For *Azospirillum*, a system of fine-tuned hormonal cross-talk also involving flagellin has been proposed to balance immunity with plant growth (Elías et al. 2022; Fukami et al. 2018; Mora et al. 2023). This means an increase in immunity does not necessarily cause a trade-off in decreased plant growth, which is important in agricultural settings. At this point in time, we do not know what the effect of our treatment is at the molecular level, but we plan a larger transcriptome study in the near future. This will determine the effect of the treatments on plant genes contributing to colonization, systemic resistance, and plant hormones, as well as genes encoding virulence factors of *P. syringae* pv. *tomato* DC3000.

Phyllosphere and rhizosphere

To extend the perspective from looking at the experiment as a tri-partite relationship between two bacterial and one plant species to viewing the tomatoes as one system, we determined the effect of our treatments on phyllosphere and rhizosphere. Comparing the microbiome of leaves to that of roots, a first noticeable difference was the extremely low level of 16S rDNA from any bacteria in leaf homogenates from un-challenged tomatoes (Fig. 5A and B). Low diversity of microbes in the tomato phyllosphere has been observed before (Dong et al. 2019) and could be due to a masking of bacterial 16S rDNA by high levels of chloroplasts (Tian et al. 2017), as was seen in our experiment (Table S1, first tab). As a general rule, an abundance of bacteria of 10^6 in leaf homogenate samples used for 16S rDNA sequencing is considered the lower level of detection (Villette et al. 2021). In root homogenates, we detected 16S rDNA in all

test groups (Figs. 7A and B). A second large difference between phyllosphere and rhizosphere was richness. In the phyllosphere, we started with 684 taxonomies, which were narrowed down to 67 after applying the ≥50 filter. In the rhizosphere, we initially obtained 8,619 taxonomies, which we narrowed down to 280, applying the much more restrictive ≥500 filter. As one similarity between the two microbiomes, Proteobacteria were the pre-dominant phylum in both.

In phyllosphere and rhizosphere, the microbial composition in our experiment was similar to previous reports, which also gave us confidence that sterilization of the growth medium at the beginning of plant growth would not interfere with the microbiome several weeks later. This is consistent with a previous study on a prairie grass, where the bacterial communities in the soil were no longer discernable between sterile and non-sterile soil after 7 weeks (Hobbs et al. 2026). Sterile growth medium was also used in one of the three studies that our experimental protocol was built upon (Bashan and De-Bashan 2002). In full agreement with the literature on the tomato microbiome, proteobacteria were the predominant phylum (Dong et al. 2019), a majority of the species belong to the Gammaproteobacteria (Romero et al. 2014). Actinobacteriota, Bacteroidota, Verrucomicrobiota, and Patescibacteria were part of the rhizosphere alongside Proteobacteria (Fagnano et al. 2025); Rhizobiales and Myxococcales were also part of the rhizosphere (Cheng et al. 2020). Most Pseudomonadales which scored high abundances in our experiment were from the genus *Pseudomonas*, which has been previously observed (Dong et al. 2019). *Sphingobium* which scored high abundances in our experiment has been described as part of the rhizosphere in response to α-tomatin (Takamatsu et al. 2023), where it produces indole 3-acetic acid (Gao et al. 2023), and catalyzes toxic steroidal glycoalkaloids (Nakayasu et al. 2023). In contradiction to the literature (Fagnano et al. 2025), we failed to identify Firmicutes.

The key part of our microbiome analysis was to characterize the effect our treatments had on phyllosphere and rhizosphere. In summary from the phyllosphere, there are three distinct outcomes of our treatments on specific bacterial orders; first, tomato seedling exudate increased the abundance of Enterobacterales in the presence of *A. brasilense* Sp7. Second, cytidine increased the abundance of Pseudomonadales, more so in the presence of *A. brasilense* Sp7. Third, there is a possibility that *A. brasilense* Sp7 decreased the abundance of Xanthomonadales in all three comparisons between a -*Abra* and a +*Abra* test group.

Members of the Xanthomonadales are often human and/or plant pathogens. A recent review article suggests the use of microorganisms for control instead of chemicals (Marin et al. 2019). As one example, *Azospirillum argentinense* was able to inhibit pathogens, while also increasing beneficial bacteria (Coniglio et al. 2022). One of two species in the Xanthomonadales and the only one that had a significant abundance is *S. maltophilia* (Supplemental Table 1), a human pathogen, causing a number of respiratory, bloodstream, and urinary tract infections (Brooke 2012). Abundance of *S. maltophilia* was reduced in the +*Abra* +Ex +Ps and +*Abra* +CYD +Ps test groups. Analyzing the remaining pathogens from the phyllosphere (Fig. 6), 16S rDNA abundances from a total of eight pathogens were decreased in the test groups +*Abra* +Ex +Ps and +*Abra* +CYD +Ps (Fig. 8). These are two species of *Enterobacter cloaceae*, a phytopathogen that causes brown necrosis on tomato leaves (Jin et al. 2022) and human pathogen, causing gastrointestinal infections, endocarditis and meningitis (Stokes et al. 2022). *Pantoea ananatis* is a major plant pathogen for several crops, including pineapple (Mergaert et al. 1993; Weller-Stuart et al. 2017), *Pantoea agglomerans* is a plant and human pathogen (Gavini et al. 1989; Shu et al. 2022). Three species of *Pseudomonas* are two rare human

pathogens (Almuzara et al. 2010; Owusu et al. 2017), and a plant pathogen causing tomato pith necrosis (Jin et al. 2023).

Intriguingly, it is the rhizosphere that has long been described as a reservoir for human pathogens, including those of the genera *Enterobacter* and *Stenotrophomonas* (Berg et al. 2005; Brooke 2012). Kim and coworkers described this transfer of human pathogens from plants as 'crossing the kingdom border' (Kim et al. 2020). In our experiments, we detected numerous pathogens in the phyllosphere.

Analyzing 16S rDNA abundance within the rhizosphere, absence or presence of *A. brasilense* Sp7 appeared to be the largest driver behind the PC1 component (Fig. 8A). Comparing data from the heatmap to those from the PCA analysis, we see a shift from Flavobacteriales, Pseudomonadales, Propionibacteriales, Saccharomonadales, Rhizobiales, Tepidisphaerales, and Abditibacteriales in the absence of the PGPR to Micrococcales, Azospirillales, Salinisphaerales, and Microtrichales in the presence of *A. brasilense* Sp7 (Figs. 8C and 9B, Table 2). We find it especially intriguing that *A. brasilense* increased the abundance of members of its own order Azospirillales, an observation that we believe has not been made before. Furthermore, this appears to go to the expense of Rhizobiales, another large group of beneficial bacteria, though with a strong host specificity for legumes (Boivin et al. 2021; Sijilmassi et al. 2020). We are asking the question whether *A. brasilense* may be the perfect PGPR for tomatoes.

Conclusion

In conclusion, the combination treatments of *A. brasilense* Sp7 and exudate or *A. brasilense* Sp7 and cytidine had major impacts on our system consisting of tomato plants and the phytopathogen

P. syringae pv. *tomato* DC3000. A primary observation is the massive reduction in disease severity caused by the pathogen. While we currently do not have a good hypothesis on the underlying reasons for this reduction, it appeared to be paralleled by an increase in the abundance of the PGPR in the presence of cytidine, which can cause a general improvement of plant health or more specific effects, which will be investigated in future experiments. We did not see a reduction in the challenge pathogen, but observed a reduction in eight plant or human pathogens on the tomato leaves. It is possible that besides a reduction in disease symptoms by our challenge pathogen, which already has positive economic consequences, our treatment may also have implications in food safety.

Acknowledgements

The authors thank Dr. Gladys Alexandre (University of Tennessee, Knoxville, TN) for providing the *A. brasilense* Sp7 strain and Dr. Melania Filiatrault (USDA/ARA, Ithaca, NY) for many helpful discussions. We thank Scott Hoselton and Kaycie Schmidt from the Dr. Thomas Glass Biotech Innovation Core at NDSU for performing the 16S rDNA analysis and helping us with the dPCR. We thank Carl Denton for editing the French version of the abstract after producing it with Copilot.

Competing Interest Statement

The authors declare there are no competing interests.

Author Contribution Statement

B.M.P. did conceptualization of the research, funding acquisition, project administration, and data curation. B.M.P. wrote the first draft of the manuscript. S.M.H. was responsible for

investigation, methodology, student supervision, and reviewing/editing. J.A.N.T., did investigation, data curation, and reviewing/editing. B.O. contributed to investigation and data analysis, and did reviewing/editing.

Data Availability Statement

All data are either included in the article or provided as online supplement.

Funding Statement

The research was funded by Specialty Crop Block Grant 22-242 from the USDA/NIFA and grant 24-2030 from the North Dakota Agricultural Products and Utilization Commission. BMP was supported, in part, by the intramural research program of the U.S. Department of Agriculture, National Institute of Food and Agriculture, Hatch project accession number, 7009493. The findings and conclusions in this preliminary publication have not been formally disseminated by the U. S. Department of Agriculture and should not be construed to represent any agency determination or policy.

Figure Legends

Fig. 1. Disease severity. For the disease assessments, we collected percent leaf death data from a minimum of 3 replicate experiments. Red boxes mark data populations for test groups that were challenged with *P. syringae* pv. *tomato* DC3000, white boxes mark data populations for un-challenged test groups. The lines within the boxes indicate the medians of the populations, the small open circles within the boxes are the data points from each individual plant. The numbers in red are the averages across the populations for challenged test groups. The blunt end line across all test groups indicates the *p*-value from the one-way ANOVA. The open end lines between two bars are the *p*-values from pairwise comparisons with the Tukey test.

Fig. 2. Abundance of *P. syringae* on tomato leaves. Panel A shows the live *Pseudomonas* counts on tomato leaves. We determined $\log_{10}$ CFU/g plant material from two phytopathogen experiments. The numbers in red are the averages across the populations for challenged test groups, numbers in black are for un-challenged test groups. Panel B shows the 16S rDNA abundance of *P. syringae* pv. *tomato* DC3000. 16S rDNA was sequenced from leaf homogenates from 3 plants. Panel C shows the number of copies of the *hrpL* gene from the same leaf homogenates by dPCR.

For all panels, red boxes mark data for test groups that were challenged with the pathogen, white boxes mark data populations for un-challenged test groups. The lines within the boxes indicate the medians of the populations, the small open circles within the boxes are the data points from each individual plant. The blunt end lines across all test groups indicate the *p*-value from the one-way ANOVA that was performed across all twelve test groups. Open end lines between two bars are *p*-values from pairwise comparisons with Tukey.

Fig. 3. Abundance of *A. brasilense* Sp7 on roots. 16S rDNA was sequenced from root homogenates from 3 plants. Floating bars in blue are from pathogen challenged test groups, floating bars in white are from un-challenged test groups. The line within the floating bars is the median of the population. The blunt end line across all test groups indicates the *p*-value from the one-way ANOVA that was performed across all twelve test groups. The open ended line between two bars is the *p*-value from pairwise comparison with Tukey.

Fig. 4. Phylogenetic tree from the tomato phyllosphere. 16S rDNA was analyzed from leaf homogenates from 3 plants. The phylogenetic tree was generated in Galaxy and visualized in iTOL from the 67 bacterial species that exhibited 16S rDNA abundances higher than 50 across all test groups and replicates.

Fig. 5. Tomato phyllosphere. Fig. 5A demonstrates richness, Fig. 5B the sum abundances across all bacterial species per test group. Fig. 5C is the heat map for mean percent 16rDNA abundances from all species within eight orders for pathogen challenged test groups. PCA analysis is presented as PC scores in Fig. 5D and Biplot in Fig. 5E.

Fig. 6. Heatmap for human or plant pathogens. We computed mean percent 16S rDNA abundances for eight species.

Fig. 7. Tomato rhizosphere, richness and abundances. Fig. 7A demonstrates richness, Fig. 7B the sum abundances across all bacterial species per test group. Fig. 7C is the heat map for mean percent 16rDNA abundances from all species within each order.

Fig. 8. PCA analysis. Fig. 8A shows the PC scores and Fig. 8B the Biplot. See Supplemental Table 5 for association strengths.

References

Alexandre, G. 2026. Chemotaxis and other forms of taxis behaviors. *In* The definitive hHandbook of *Azospirillum*: 100 Years of research and application around the world. *Edited by* F.D. Cassán and L. de Bashan and F. Wisniewski-Dyé and G. A. Maroniche. Springer Nature Switzerland, Cham. pp. 111-125.

Alexandre, G., Greer, S.E., and Zhulin, I.B. 2000. Energy taxis is the dominant behavior in *Azospirillum brasilense*. J. Bacteriol. **182**(21): 6042-6048. doi:doi:10.1128/JB.182.21.6042-6048.2000.

Almuzara, M.N., Vazquez, M., Tanaka, N., Turco, M., Ramirez, M.S., Lopez, E.L., Pasteran, F., Rapoport, M., Procopio, A., and Vay, C.A. 2010. First case of human infection due to *Pseudomonas fulva*, an environmental bacterium isolated from cerebrospinal fluid. J Clin Microbiol **48**(2): 660-664. doi:doi:10.1128/jcm.01849-09.

Baatsen, J., Hosaka, G.K., Mondin, M., Azevedo, J.L., Hungria, M., and Quecine, M.C. 2025. Benzoxazinoids stimulate chemotaxis and act as a signaling molecule in *Azospirillum brasilense* Ab-V5, while showing minor effects on *Pseudomonas protegens* Pf-5. mBio **16**(9): e0141425. doi:10.1128/mbio.01414-25.

Bashan, Y., and De-Bashan, L.E. 2002. Protection of tomato seedlings against infection by *Pseudomonas syringae* pv. *tomato* by using the plant growth-promoting bacterium *Azospirillum brasilense*. Appl Environ Microbiol **68**(6): 2637-2643. doi:10.1128/aem.68.6.2637-2643.2002.

Berg, G., Eberl, L., and Hartmann, A. 2005. The rhizosphere as a reservoir for opportunistic human pathogenic bacteria. Environmental Microbiology **7**(11): 1673-1685. doi:https://doi.org/10.1111/j.1462-2920.2005.00891.x.

Bergougnoux, V. 2014. The history of tomato: from domestication to biopharming. Biotechnol Adv **32**(1): 170-189. doi:10.1016/j.biotechadv.2013.11.003.

Beringer, J.E. 1974. R factor transfer in *Rhizobium leguminosarum*. Microbiology **84**(1): 188-198. doi:doi: 10.1099/00221287-84-1-188.

Boivin, S., Mahé, F., Debellé, F., Pervent, M., Tancelin, M., Tauzin, M., Wielbo, J., Mazurier, S., Young, P., and Lepetit, M. 2021. Genetic variation in host-specific competitiveness of the symbiont *Rhizobium leguminosarum* Symbiovar *viciae*. Front Plant Sci **12**: 719987. doi:10.3389/fpls.2021.719987.

Botta, A.L., Santacecilia, A., Ercole, C., Cacchio, P., and Del Gallo, M. 2013. *In vitro* and *in vivo* inoculation of four endophytic bacteria on *Lycopersicon esculentum*. N Biotechnol **30**(6): 666-674. doi:10.1016/j.nbt.2013.01.001.

Brooke, J.S. 2012. *Stenotrophomonas maltophilia*: an emerging global opportunistic pathogen. Clinical microbiology reviews **25**(1): 2-41. doi:10.1128/cmr.00019-11.

Buell, C.R., Joardar, V., Lindeberg, M., Selengut, J., Paulsen, I.T., Gwinn, M.L., Dodson, R.J., Deboy, R.T., Durkin, A.S., Kolonay, J.F., Madupu, R., Daugherty, S., Brinkac, L., Beanan, M.J., Haft, D.H., Nelson, W.C., Davidsen, T., Zafar, N., Zhou, L., Liu, J., Yuan, Q., Khouri, H., Fedorova, N., Tran, B., Russell, D., Berry, K., Utterback, T., Van Aken, S.E., Feldblyum, T.V., D'Ascenzo, M., Deng, W.L., Ramos, A.R., Alfano, J.R., Cartinhour, S., Chatterjee, A.K., Delaney, T.P., Lazarowitz, S.G., Martin, G.B., Schneider, D.J., Tang, X., Bender, C.L., White, O., Fraser, C.M., and Collmer, A. 2003. The complete genome sequence of the *Arabidopsis* and tomato pathogen *Pseudomonas*

syringae pv. *tomato* DC3000. Proc Natl Acad Sci U S A **100**(18): 10181-10186. doi:10.1073/pnas.1731982100.

Cassán, F., Vanderleyden, J., and Spaepen, S. 2014. Physiological and agronomical aspects of phytohormone production by model plant-growth-promoting rhizobacteria (PGPR) belonging to the genus *Azospirillum*. J Plant Growth Regul **33**(2): 440-459.

Cassán, F., Maroniche, G., Reis, V.M., Etto, R.M., Bellotti, G., Alexandre, G., Torres, D., Nievas, S., Tripathi, A.K., Perez, R., de Souza, E.M., Pineda, E.G., Pedraza, R., Peña, E.M.B., Gureeva, M., Prigent-Combaret, C., Díaz-Zorita, M., Vio, S.A., Del Gallo, M., Buttrós, V.H., de Oliveira Pedrosa, F., Puente, M., García, J.E., López, B., Palacios, O., Wisniewski-Dyé, F., and de-Bashan, L. 2026. A century of research on *Azospirillum* and still so much to discover. Plant and Soil. doi:10.1007/s11104-025-08178-9.

Cassán, F.D.d.B., L.; Wisniewski-Dyé, F.; Maroniche, G.A. 2026. The definitive handbook of *Azospirillum*. Springer.

Cerna-Vargas, J.P., Santamaría-Hernando, S., Matilla, M.A., Rodríguez-Herva, J.J., Daddaoua, A., Rodríguez-Palenzuela, P., Krell, T., and López-Solanilla, E. 2019. Chemoperception of specific amino acids controls phytopathogenicity in *Pseudomonas syringae* pv. tomato. mBio **10**(5). doi:10.1128/mBio.01868-19.

Chakravarthy, S., Butcher, B.G., Liu, Y., D'Amico, K., Coster, M., and Filiatrault, M.J. 2017. Virulence of *Pseudomonas syringae* pv. tomato DC3000 Is influenced by the catabolite repression control protein Crc. Mol Plant Microbe Interact **30**(4): 283-294. doi:10.1094/mpmi-09-16-0196-r.

Cheng, Z., Lei, S., Li, Y., Huang, W., Ma, R., Xiong, J., Zhang, T., Jin, L., Haq, H.U., Xu, X., and Tian, B. 2020. Revealing the variation and stability of bacterial communities in tomato rhizosphere microbiota. Microorganisms **8**(2). doi:10.3390/microorganisms8020170.

Compant, S., Cassan, F., Kostić, T., Johnson, L., Brader, G., Trognitz, F., and Sessitsch, A. 2025. Harnessing the plant microbiome for sustainable crop production. Nature Rev Microbiol **23**(1): 9-23. doi:10.1038/s41579-024-01079-1.

Coniglio, A., Larama, G., Molina, R., Mora, V., Torres, D., Marin, A., Avila, A.I., Lede NoirCarlan, C., Erijman, L., and Figuerola, E.L. 2022. Modulation of maize rhizosphere microbiota composition by inoculation with *Azospirillum argentinense* Az39 (formerly *A. brasilense* Az39). J Soil Sci Plant Nutr **22**(3): 3553-3567.

Contreras-Cornejo, H.A., Sanchez-Yanez, J.M.; Carrillo-Flores, E.; Mellado-Rojas, Ma.E.; Berltran-Pena, E.M. 2026. Interaction of *Azospirillum* ssp. with plants; molecular plant growth responses. *In* The definitive hHandbook of *Azospirillum*: 100 Years of research and application around the world. *Edited by* F.D. Cassán and L. de Bashan and F. Wisniewski-Dyé and G. A. Maroniche. Springer Nature Switzerland, Cham. pp. 323-342.

da Cunha, E.T., Pedrolo, A.M., Paludo, F., Scariot, M.C., and Arisi, A.C.M. 2020. *Azospirillum brasilense* viable cells enumeration using propidium monoazide-quantitative PCR. Arch Microbiol **202**(7): 1653-1662. doi:10.1007/s00203-020-01877-0.

Dong, C.-J., Wang, L.-L., Li, Q., and Shang, Q.-M. 2019. Bacterial communities in the rhizosphere, phyllosphere and endosphere of tomato plants. PloS one **14**(11): e0223847.

El-Beltagi, H.S., Ahmad, I., Basit, A., Abd El-Lateef, H.M., Yasir, M., Tanveer Shah, S., Ullah, I., Elsayed Mohamed Mohamed, M., Ali, I., Ali, F., Ali, S., Aziz, I., Kandeel, M., and Zohaib Ikram, M. 2022. Effect of *Azospirillum* and *Azotobacter* species on the

performance of cherry tomato under different salinity levels. Gesunde Pflanzen **74**(2): 487-499. doi:doi:10.1007/s10343-022-00625-2.

El-Fatah, B., Imran, M., Abo-Elyousr, K.A.M., and Mahmoud, A.F. 2023. Isolation of *Pseudomonas syringae* pv. tomato strains causing bacterial speck disease of tomato and marker-based monitoring for their virulence. Mol Biol Rep **50**(6): 4917-4930. doi:10.1007/s11033-023-08302-x.

Elías, J.M., Ramírez-Mata, A., Albornóz, P.L., Baca, B.E., Díaz-Ricci, J.C., and Pedraza, R.O. 2022. The polar flagellin of *Azospirillum brasilense* REC3 induces a defense response in strawberry plants against the fungus *Macrophomina phaseolina*. J Plant Gro Regul **41**(7): 2992-3008. doi:10.1007/s00344-021-10490-4.

Elsharkawy, M.M., Khedr, A.A., Mehiar, F., El-Kady, E.M., Alwutayd, K.M., and Behiry, S.I. 2023. Rhizobacterial colonization and management of bacterial speck pathogen in tomato by *Pseudomonas* spp. Microorganisms **11**(5). doi:10.3390/microorganisms11051103.

Eskew, D.F., D.D. 1977. Nitrogen fixation, denitrification, and pleomorphic growth in a highly pigmented *Spirillum lipoferum*. Appl. Environ. Microbiol. **34**: 582-585. doi:doi: 10.1128/aem.34.5.582-585.1977.

Fagnano, F.M., Ventorino, V., Pasolli, E., Romano, I., Ambrosino, P., and Pepe, O. 2025. From microbiome to biostimulants: unlocking the potential of tomato root endophytes. BMC Plant Biol **25**(1): 427. doi:10.1186/s12870-025-06447-4.

Feng, Z., Liang, Q., Yao, Q., Bai, Y., and Zhu, H. 2024. The role of the rhizobiome recruited by root exudates in plant disease resistance: current status and future directions. Environ Microbiome **19**(1): 91. doi:10.1186/s40793-024-00638-6.

Fukami, J., de la Osa, C., Ollero, F.J., Megías, M., and Hungria, M. 2018. Co-inoculation of maize with *Azospirillum brasilense* and *Rhizobium tropici* as a strategy to mitigate salinity stress. Funct Plant Biol **45**(3): 328-339. doi:10.1071/fp17167.

Ganusova, E.E., Russell, M.H., Patel, S., Seats, T., and Alexandre, G. 2024. An *Azospirillum brasilense* chemoreceptor that mediates nitrate chemotaxis has conditional roles in the colonization of plant roots. Appl Environ Microbiol **90**(6): e0076024. doi:10.1128/aem.00760-24.

Ganusova, E.E., Vo, L.T., Abraham, P.E., O'Neal Yoder, L., Hettich, R.L., and Alexandre, G. 2021. The *Azospirillum brasilense* core chemotaxis proteins CheA1 and CheA4 link chemotaxis signaling with nitrogen metabolism. mSystems **6**(1). doi:10.1128/mSystems.01354-20.

Ganusova, E.E., Rost, M., Aksenova, A., Abdulhussein, M., Holden, A., and Alexandre, G. 2023. *Azospirillum brasilense* AerC and Tlp4b cytoplasmic chemoreceptors are promiscuous and interact with the two membrane-bound chemotaxis signaling clusters mediating chemotaxis responses. J Bacteriol **205**(6): e0048422. doi:10.1128/jb.00484-22.

Gao, R., Dong, H., Liu, Y., Yao, Q., Li, H., and Zhu, H. 2023. *Sphingomonas lycopersici* sp. *nov*., isolated from tomato rhizosphere soil. Int J Syst Evol Microbiol **73**(5). doi:10.1099/ijsem.0.005920.

Gavini, F., Mergaert, J., Beji, A., Mielcarek, C., Izard, D., Kersters, K., and De Ley, J. 1989. Transfer of *Enterobacter agglomerans* (Beijerinck 1888) Ewing and Fife 1972 to *Pantoea* gen. *nov*. as *Pantoea agglomerans* comb, *nov*. and description of *Pantoea dispersa* sp. *nov*. Internat J System Evolut Microbiol **39**(3): 337-345.

Hobbs, A., Ochoa-Rojas, D., Humphrey, C.E., Kyndt, J.A., and Moore, T.C. 2026. Soil microbiome perturbation impedes growth of Bouteloua curtipendula and increases

relative abundance of soil microbial pathogens. PLoS One **21**(1): e0312218. doi:10.1371/journal.pone.0312218.

Housh, A.B., Noel, R., Powell, A., Waller, S., Wilder, S.L., Sopko, S., Benoit, M., Powell, G., Schueller, M.J., and Ferrieri, R.A. 2023. Studies Using Mutant Strains of Azospirillum brasilense Reveal That Atmospheric Nitrogen Fixation and Auxin Production Are Light Dependent Processes. Microorganisms **11**(7): 1727. Available from https://www.mdpi.com/2076-2607/11/7/1727 [accessed.

Huang, J., Zhu, L., Lu, X., Cui, F., Wang, J., and Zhou, C. 2023. A simplified synthetic rhizosphere bacterial community steers plant oxylipin pathways for preventing foliar phytopathogens. Plant Physiol Biochem **202**: 107941. doi:10.1016/j.plaphy.2023.107941.

Janda, M., Rybak, K., Krassini, L., Meng, C., Feitosa-Junior, O., Stigliano, E., Szulc, B., Sklenar, J., Menke, F.L.H., Malone, J.G., Brachmann, A., Klingl, A., Ludwig, C., and Robatzek, S. 2023. Biophysical and proteomic analyses of *Pseudomonas syringae* pv. *tomato* DC3000 extracellular vesicles suggest adaptive functions during plant infection. mBio **14**(4): e0358922. doi:10.1128/mbio.03589-22.

Jin, Y., Wu, X., Sa, R., Dong, H., Xiong, Y., He, S., Li, C., and Geng, X. 2022. First report of *Enterobacter cloacae* causing stem, leaf and fruit rot on tomato in China. Plant Dis. doi:10.1094/pdis-08-22-1749-pdn.

Jin, Y., Wu, X., Sa, R., Dong, H., Xiong, Y., He, S., Li, C., and Geng, X. 2023. First report of *Enterobacter cloacae* causing stem, leaf, and fruit rot on tomato in China. Plant Disease **107**(6): 1936. doi:10.1094/pdis-08-22-1749-pdn.

Johnsen, K., and Nielsen, P. 1999. Diversity of *Pseudomonas* strains isolated with King's B and Gould's S1 agar determined by repetitive extragenic palindromic-polymerase chain reaction, 16S rDNA sequencing and Fourier transform infrared spectroscopy characterisation. FEMS Microbiol Lett **173**(1): 155-162. doi:10.1111/j.1574-6968.1999.tb13497.x.

Kim, J.S., Yoon, S.J., Park, Y.J., Kim, S.Y., and Ryu, C.M. 2020. Crossing the kingdom border: Human diseases caused by plant pathogens. Environ Microbiol **22**(7): 2485-2495. doi:10.1111/1462-2920.15028.

King, E.O., Ward, M.K., and Raney, D.E. 1954. Two simple media for the demonstration of pyocyanin and fluorescin. J Lab Clin Med **44**(2): 301-307.

King, W.L., Grandinette, E.M., Trase, O., Rolon, M.L., Salis, H.M., Wood, H., and Bell, T.H. 2024. Autoclaving is at least as effective as gamma irradiation for biotic clearing and intentional microbial recolonization of soil. mSphere **9**(7): e00476-00424. doi:doi:10.1128/msphere.00476-24.

Korenblum, E., Dong, Y., Szymanski, J., Panda, S., Jozwiak, A., Massalha, H., Meir, S., Rogachev, I., and Aharoni, A. 2020. Rhizosphere microbiome mediates systemic root metabolite exudation by root-to-root signaling. Proc Natl Acad Sci U S A **117**(7): 3874-3883. doi:10.1073/pnas.1912130117.

Lindeberg, M., Biehl, B.S., Glasner, J.D., Perna, N.T., Collmer, A., and Collmer, C.W. 2009. Gene ontology annotation highlights shared and divergent pathogenic strategies of type III effector proteins deployed by the plant pathogen *Pseudomonas syringae* pv *tomato* DC3000 and animal pathogenic *Escherichia coli strains*. BMC Microbiol **9 Suppl 1**(Suppl 1): S4. doi:10.1186/1471-2180-9-s1-s4.

Ma, L.J., Geiser, D.M., Proctor, R.H., Rooney, A.P., O'Donnell, K., Trail, F., Gardiner, D.M., Manners, J.M., and Kazan, K. 2013. *Fusarium* pathogenomics. Annu Rev Microbiol **67**: 399-416. doi:10.1146/annurev-micro-092412-155650.

Ma, S., Chen, Q., Zheng, Y., Ren, T., He, R., Cheng, L., Zou, P., Jing, C., Zhang, C., and Li, Y. 2025. A tale for two roles: Root-secreted methyl ferulate inhibits *P. nicotianae* and enriches the rhizosphere *Bacillus* against black shank disease in tobacco. Microbiome **13**(1): 33. doi:10.1186/s40168-024-02008-3.

Marin, V.R., Ferrarezi, J.H., Vieira, G., and Sass, D.C. 2019. Recent advances in the biocontrol of *Xanthomonas* spp. World J Microbiol Biotechnol **35**(5): 72. doi:10.1007/s11274-019-2646-5.

Mergaert, J., Verdonck, L., and Kersters, K. 1993. Transfer of *Erwinia ananas* (synonym, *Erwinia uredovora*) and *Erwinia stewartii* to the genus *Pantoea emend*. as *Pantoea ananas* (Serrano 1928) comb. *nov*. and Pantoea stewartii (Smith 1898) comb. *nov*., respectively, and description of *Pantoea stewartii* subsp. *indologenes* subsp. *nov*. Internat J System Evol Microbiol **43**(1): 162-173.

Mora, V., López, G., Molina, R., Coniglio, A., Nievas, S., De Diego, N., Zeljković, S.Ć., Sarmiento, S.S., Spíchal, L., Robertson, S., Wilkins, O., Elías, J., Pedraza, R., Estevez, J.M., Belmonte, M.F., and Cassán, F. 2023. *Azospirillum argentinense* modifies *Arabidopsis* root architecture through auxin-dependent pathway and flagellin. Journal of Soil Science and Plant Nutrition **23**(3): 4543-4557. doi:10.1007/s42729-023-01371-8.

Nakayasu, M., Takamatsu, K., Yazaki, K., and Sugiyama, A. 2022. Plant specialized metabolites in the rhizosphere of tomatoes: secretion and effects on microorganisms. Biosci Biotechnol Biochem **87**(1): 13-20. doi:10.1093/bbb/zbac181.

Nakayasu, M., Ohno, K., Takamatsu, K., Aoki, Y., Yamazaki, S., Takase, H., Shoji, T., Yazaki, K., and Sugiyama, A. 2021. Tomato roots secrete tomatine to modulate the bacterial assemblage of the rhizosphere. Plant Physiol **186**(1): 270-284. doi:10.1093/plphys/kiab069.

Nakayasu, M., Takamatsu, K., Kanai, K., Masuda, S., Yamazaki, S., Aoki, Y., Shibata, A., Suda, W., Shirasu, K., Yazaki, K., and Sugiyama, A. 2023. Tomato root-associated *Sphingobium* harbors genes for catabolizing toxic steroidal glycoalkaloids. mBio **14**(5): e0059923. doi:10.1128/mbio.00599-23.

Namgung, M., Lim, Y.J., Kang, M.K., Oh, C.S., and Park, D.H. 2019. *Pseudomonas syringae* pv. *tomato* DC3000 improves *Escherichia coli* O157:H7 survival in tomato plants. J Microbiol Biotechnol **29**(12): 1975-1981. doi:10.4014/jmb.1907.07072.

Nievas, S., Coniglio, A., Takahashi, W.Y., López, G.A., Larama, G., Torres, D., Rosas, S., Etto, R.M., Galvão, C.W., Mora, V., and Cassán, F. 2023. Unraveling *Azospirillum*'s colonization ability through microbiological and molecular evidence. J Appl Microbiol **134**(4). doi:10.1093/jambio/lxad071.

Nisha, F.A., Horne, S.M., and Prüß, B.M. 2025. *Azospirillum brasilense* and cytidine enhance lateral roots of peas. FEMS Microbiol Lett **372**: fnaf025. doi:10.1093/femsle/fnaf025.

Nisha, F.A., Tagoe, J.N.A., Pease, A.B., Horne, S.M., Ugrinov, A., Geddes, B.A., and Prüß, B.M. 2024. Plant seedlings of peas, tomatoes, and cucumbers exude compounds that are needed for growth and chemoattraction of *Rhizobium leguminosarum* bv. *viciae* 3841 and *Azospirillum brasilense* Sp7. Can J Microbiol **70**(5): 150-162. doi:10.1139/cjm-2023-0217.

Owusu, M., Owusu-Dabo, E., Acheampong, G., Osei, I., Amuasi, J., Sarpong, N., Annan, A., Chiang, H.-Y., Kuo, C.-H., Park, S.E., Marks, F., and Adu-Sarkodie, Y. 2017. *Pseudomonas oryzihabitans* sepsis in a 1-year-old child with multiple skin rashes: a case report. J Med Case Rep **11**(1): 77. doi:10.1186/s13256-017-1230-6.

Pellegrini, M., Ercole, C., Di Zio, C., Matteucci, F., Pace, L., and Del Gallo, M. 2020. *In vitro* and *in planta* antagonistic effects of plant growth-promoting rhizobacteria consortium against soilborne plant pathogens of *Solanum tuberosum* and *Solanum lycopersicum*. FEMS Microbiol. Lett. **367**(13). doi:doi:10.1093/femsle/fnaa099.

Peňázová, E., Dvořák, M., Ragasová, L., Kiss, T., Pečenka, J., Čechová, J., and Eichmeier, A. 2020. Multiplex real-time PCR for the detection of *Clavibacter michiganensis* subsp. *michiganensis*, *Pseudomonas syringae* pv. *tomato* and pathogenic *Xanthomonas* species on tomato plants. PLoS One **15**(1): e0227559. doi:10.1371/journal.pone.0227559.

Pereg-Gerk, L., Paquelin, A., Gounon, P., Kennedy, I.R., and Elmerich, C. 1998. A transcriptional regulator of the LuxR-UhpA family, FlcA, controls flocculation and wheat root surface colonization by *Azospirillum brasilense* Sp7. Mol Plant Microbe Interact **11**(3): 177-187. doi:10.1094/mpmi.1998.11.3.177.

Querejeta, G.A. 2023. Sterilize methods comparison for soils: cost, time, and efficiency. Internat J Methodol **2**(1): 34-40. doi:10.21467/ijm.2.1.6263.

Reddy Priya, P., Selastin Antony, R., Gopalaswamy, G., and Balachandar, D. 2016. Development of sequence-characterized amplified region (SCAR) markers as a quality standard of inoculants based on *Azospirillum*. Arch Microbiol **198**(3): 257-267. doi:10.1007/s00203-016-1187-7.

Romero, F.M., Marina, M., and Pieckenstain, F.L. 2014. The communities of tomato (*Solanum lycopersicum L.*) leaf endophytic bacteria, analyzed by 16S-ribosomal RNA gene pyrosequencing. FEMS Microbiol Lett **351**(2): 187-194. doi:10.1111/1574-6968.12377.

Santamaría-Hernando, S., López-Maroto, Á., Galvez-Roldán, C., Munar-Palmer, M., Monteagudo-Cascales, E., Rodríguez-Herva, J.J., Krell, T., and López-Solanilla, E. 2022. *Pseudomonas syringae* pv. *tomato* infection of tomato plants is mediated by GABA and l-Pro chemoperception. Mol Plant Pathol **23**(10): 1433-1445. doi:10.1111/mpp.13238.

Shu, R., Yin, X., Long, Y., Yuan, J., and Zhou, H. 2022. Detection and control of *Pantoea agglomerans* causing plum bacterial shot-hole disease by loop-mediated isothermal amplification technique. Frontiers in microbiology **13**: 896567. doi:10.3389/fmicb.2022.896567.

Sijilmassi, B., Filali-Maltouf, A., Boulahyaoui, H., Kricha, A., Boubekri, K., Udupa, S., Kumar, S., and Amri, A. 2020. Assessment of genetic diversity and symbiotic efficiency of selected Rhizobia strains nodulating lentil (*Lens culinaris* Medik.). Plants (Basel) **10**(1). doi:10.3390/plants10010015.

Steenhoudt, O., and Vanderleyden, J. 2000. *Azospirillum*, a free-living nitrogen-fixing bacterium closely associated with grasses: genetic, biochemical and ecological aspects. FEMS Microbiol Rev **24**(4): 487-506.

Stokes, W., Peirano, G., Matsumara, Y., Nobrega, D., and Pitout, J.D.D. 2022. Population-based surveillance of *Enterobacter cloacae* complex causing blood stream infections in a centralized Canadian region. European journal of clinical microbiology & infectious diseases : official publication of the European Society of Clinical Microbiology **41**(1): 119-125. doi:10.1007/s10096-021-04309-z.

Takamatsu, K., Toyofuku, M., Okutani, F., Yamazaki, S., Nakayasu, M., Aoki, Y., Kobayashi, M., Ifuku, K., Yazaki, K., and Sugiyama, A. 2023. α-Tomatine gradient across artificial roots recreates the recruitment of tomato root-associated *Sphingobium*. Plant Direct **7**(12): e550. doi:10.1002/pld3.550.

Tian, X., Shi, Y., Geng, L., Chu, H., Zhang, J., Song, F., Duan, J., and Shu, C. 2017. Template preparation affects 16S rRNA high-throughput sequencing analysis of phyllosphere microbial communities. Front Plant Sci **8**: 1623.

Vazquez, A., Zawoznik, M., Benavides, M.P., and Groppa, M.D. 2021. *Azospirillum brasilense* Az39 restricts cadmium entrance into wheat plants and mitigates cadmium stress. Plant Sci. **312**: 111056. doi:doi:10.1016/j.plantsci.2021.111056.

Vidotti, M.S., Matias, F.I., Alves, F.C., Pérez-Rodríguez, P., Beltran, G.A., Burgueño, J., Crossa, J., and Fritsche-Neto, R. 2019. Maize responsiveness to *Azospirillum brasilense*: Insights into genetic control, heterosis and genomic prediction. PLoS One **14**(6): e0217571. doi:doi:10.1371/journal.pone.0217571.

Villette, R., Autaa, G., Hind, S., Holm, J.B., Moreno-Sabater, A., and Larsen, M. 2021. Refinement of 16S rRNA gene analysis for low biomass biospecimens. Sci Rep **11**(1): 10741. doi:10.1038/s41598-021-90226-2.

Wang, H., Jin, H., Chen, Z., Li, W., Ma, J., Hu, T., Liu, Q., Zhang, Y., Lin, X., and Xie, Z. 2024. *Azospirillum isscasi* sp. nov., a bacterium isolated from rhizosphere soil of rice. Int J Syst Evol Microbiol **74**(1). doi:10.1099/ijsem.0.006218.

Wei, H.L., and Collmer, A. 2018. Defining essential processes in plant pathogenesis with *Pseudomonas syringae* pv. *tomato* DC3000 disarmed polymutants and a subset of key type III effectors. Mol Plant Pathol **19**(7): 1779-1794. doi:10.1111/mpp.12655.

Weller-Stuart, T., De Maayer, P., and Coutinho, T. 2017. *Pantoea ananatis*: genomic insights into a versatile pathogen. Mol Plant Pathol **18**(9): 1191-1198. doi:10.1111/mpp.12517.

Wen, T., Xie, P., Liu, H., Liu, T., Zhao, M., Yang, S., Niu, G., Hale, L., Singh, B.K., Kowalchuk, G.A., Shen, Q., and Yuan, J. 2023. Tapping the rhizosphere metabolites for the prebiotic control of soil-borne bacterial wilt disease. Nat Commun **14**(1): 4497. doi:10.1038/s41467-023-40184-2.

Whalen, M.C., Innes, R.W., Bent, A.F., and Staskawicz, B.J. 1991. Identification of *Pseudomonas syringae* pathogens of *Arabidopsi*s and a bacterial locus determining avirulence on both *Arabidopsis* and soybean. Plant Cell **3**(1): 49-59. doi:10.1105/tpc.3.1.49.

Xin, X.F., and He, S.Y. 2013. *Pseudomonas syringae* pv. tomato DC3000: a model pathogen for probing disease susceptibility and hormone signaling in plants. Annu Rev Phytopathol **51**: 473-498. doi:10.1146/annurev-phyto-082712-102321.

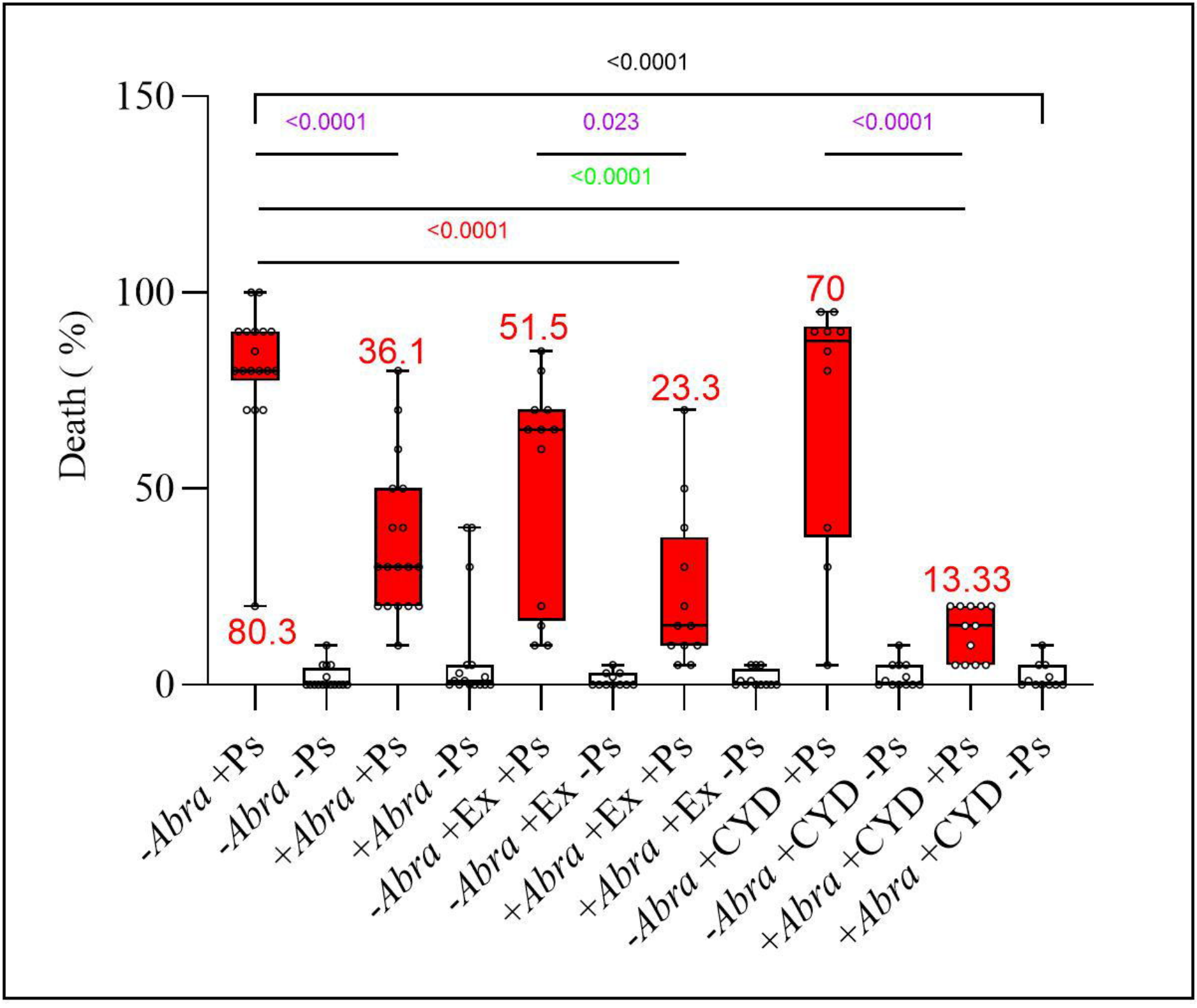
Death (%)
150
100
50
0
<0.0001
<0.0001
0.023
<0.0001
<0.0001
<0.0001
80.3
36.1
51.5
23.3
70
13.33
-Abra +Ps
-Abra -Ps
+Abra +Ps
+Abra -Ps
-Abra +Ex +Ps
-Abra +Ex -Ps
+Abra +Ex +Ps
+Abra +Ex -Ps
-Abra +CYD +Ps
-Abra +CYD -Ps
+Abra +CYD +Ps
+Abra +CYD -Ps

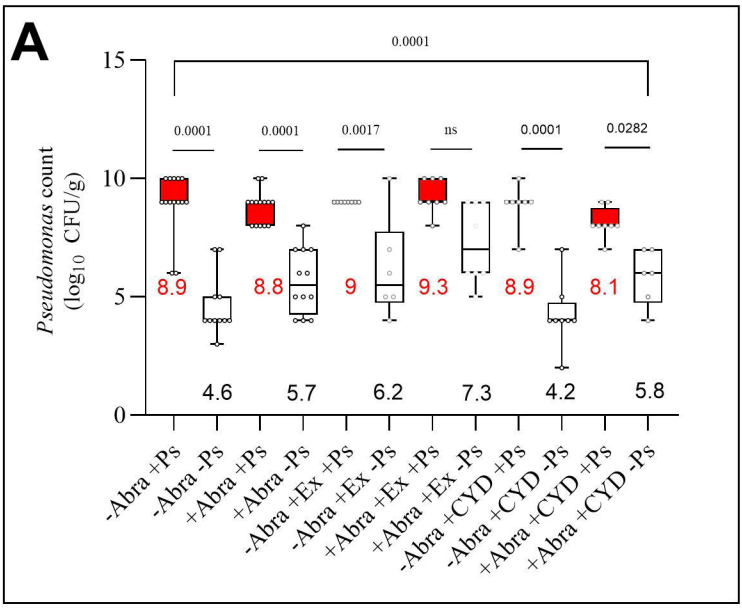
A
0.0001
0.0001
0.0001
0.0017
ns
0.0001
0.0282
Pseudomonas count
(log10 CFU/g)
15
10
5
0
8.9
8.8
9
9.3
8.9
8.1
4.6
5.7
6.2
7.3
4.2
5.8
-Abra +Ps
-Abra -Ps
+Abra +Ps
+Abra -Ps
-Abra +Ex +Ps
-Abra +Ex -Ps
+Abra +Ex +Ps
+Abra +Ex -Ps
-Abra +CYD +Ps
-Abra +CYD -Ps
+Abra +CYD +Ps
+Abra +CYD -Ps

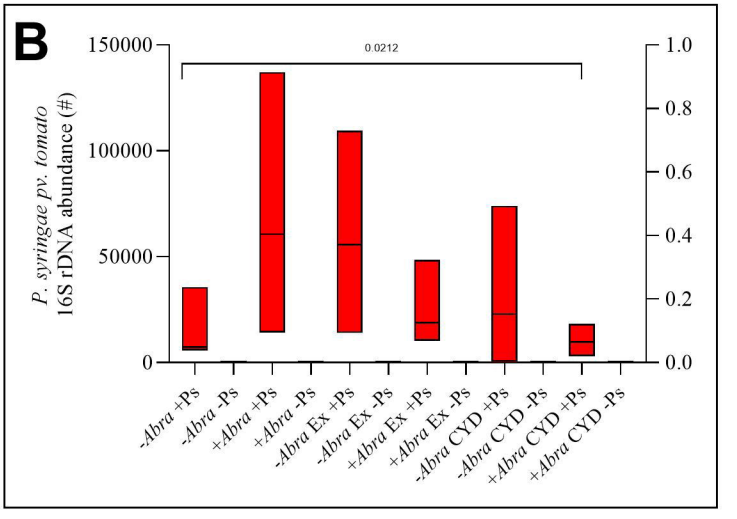
B
0.0212
P. syringae pv. tomato
16S rDNA abundance (#)
150000
100000
50000
0
1.0
0.8
0.6
0.4
0.2
0.0
-Abra +Ps
-Abra -Ps
+Abra +Ps
+Abra -Ps
-Abra Ex +Ps
-Abra Ex -Ps
+Abra Ex +Ps
+Abra Ex -Ps
-Abra CYD +Ps
-Abra CYD -Ps
+Abra CYD +Ps
+Abra CYD -Ps

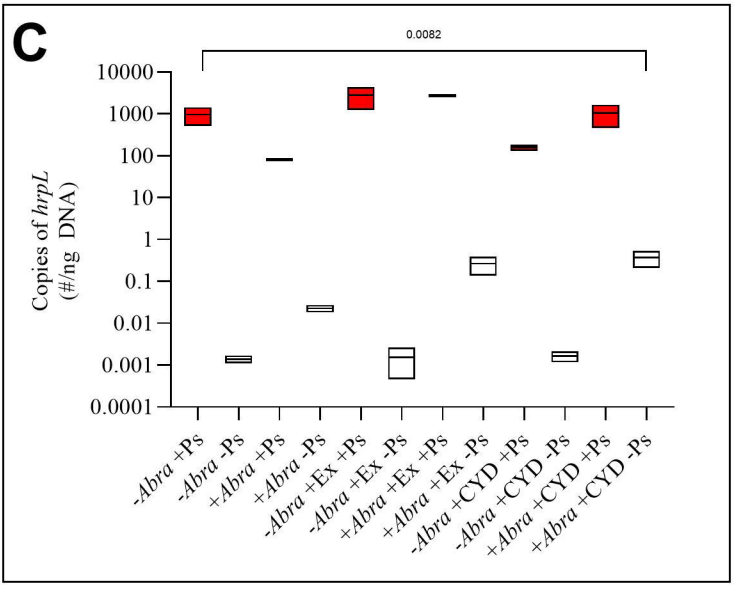
C
0.0082
Copies of hrpL
(#/ng DNA)
10000
1000
100
10
1
0.1
0.01
0.001
0.0001
-Abra +Ps
-Abra -Ps
+Abra +Ps
+Abra -Ps
-Abra +Ex +Ps
-Abra +Ex -Ps
+Abra +Ex +Ps
+Abra +Ex -Ps
-Abra +CYD +Ps
-Abra +CYD -Ps
+Abra +CYD +Ps
+Abra +CYD -Ps

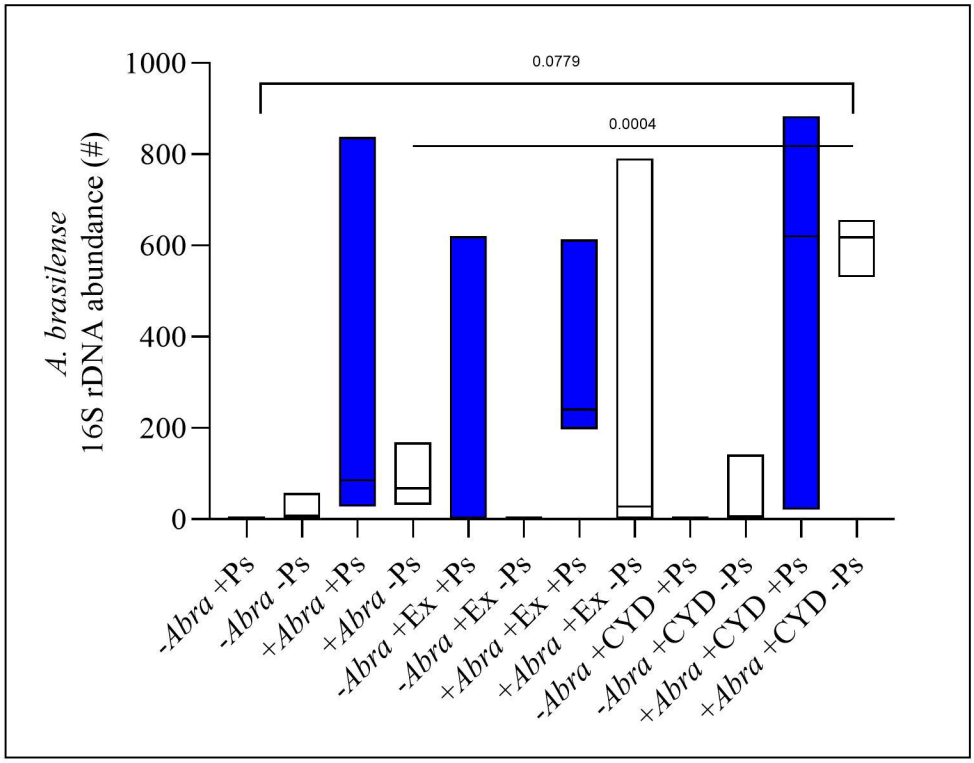
0.0779
0.0004
1000
800
600
400
200
0
A. brasilense
16S rDNA abundance (#)
-Abra +Ps
-Abra -Ps
+Abra +Ps
+Abra -Ps
-Abra +Ex +Ps
-Abra +Ex -Ps
+Abra +Ex +Ps
+Abra +Ex -Ps
-Abra +CYD +Ps
-Abra +CYD -Ps
+Abra +CYD +Ps
+Abra +CYD -Ps

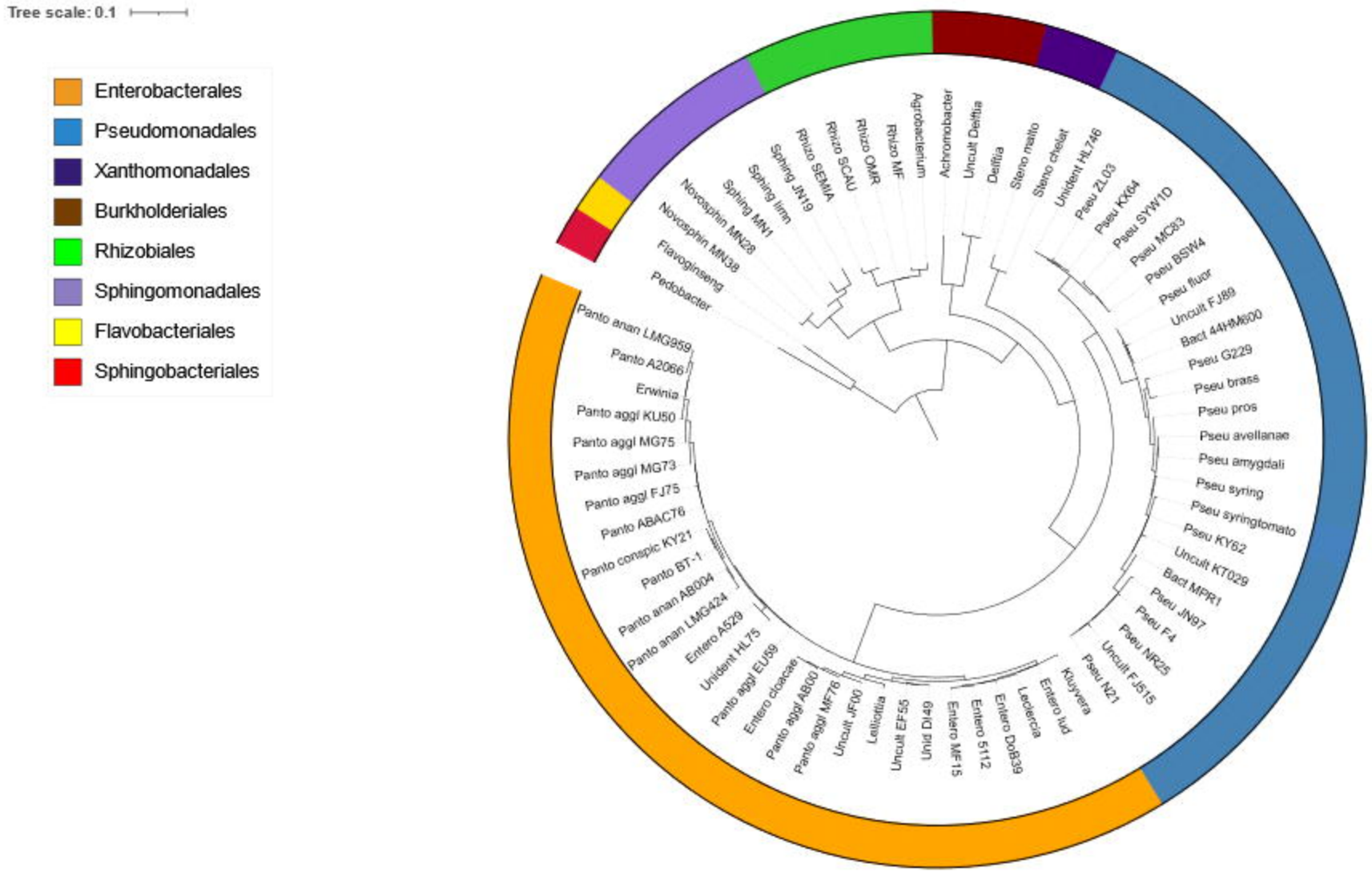
Tree scale: 0.1
Enterobacterales
Pseudomonadales
Xanthomonadales
Burkholderiales
Rhizobiales
Sphingomonadales
Flavobacteriales
Sphingobacteriales
Agrobacterium
Achromobacter
Uncult Delftia
Delftia
Steno maito
Steno chelat
Unident HL746
Pseu ZL03
Pseu KX64
Pseu SYW1D
Pseu MC83
Pseu BSW4
Pseu fluor
Uncult FJ89
Bact 44HM600
Pseu G229
Pseu brass
Pseu pros
Pseu avellanae
Pseu amygdali
Pseu syring
Pseu syringlomato
Pseu KY62
Uncult KT029
Bact MPR1
Pseu JN97
Pseu F4
Pseu NR25
Uncult FJ515
Pseu N21
Kluyvera
Entero hvd
Leclercia
Entero DoB39
Entero 5112
Entero MF15
Uncl DI49
Uncult EF56
Lelliottia
Uncult JF00
Panto aggl AB00
Panto aggl MF76
Entero cloacae
Panto aggl EU59
Unident HL75
Entero A529
Panto anan LMG424
Panto anan AB004
Panto BT-1
Panto conspic KY21
Panto ABAC76
Panto aggl FJ75
Panto aggl MG73
Panto aggl MG75
Panto aggl KU50
Erwinia
Panto A2066
Panto anan LMG959
Pedobacter
Flavoginseng
Novosphin MN38
Novosphin MN28
Sphing MN1
Sphing limn
Sphing JN19
Rhizo SEMIA
Rhizo SCAU
Rhizo OMR
Rhizo MF

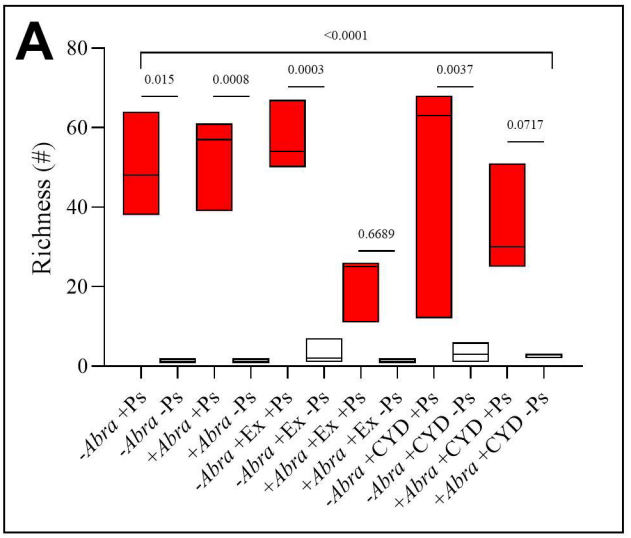
A
Richness (#)
<0.0001
0.015
0.0008
0.0003
0.6689
0.0037
0.0717
-Abra +Ps
-Abra -Ps
+Abra +Ps
+Abra -Ps
-Abra +Ex +Ps
-Abra +Ex -Ps
+Abra +Ex +Ps
+Abra +Ex -Ps
-Abra +CYD +Ps
-Abra +CYD -Ps
+Abra +CYD +Ps
+Abra +CYD -Ps

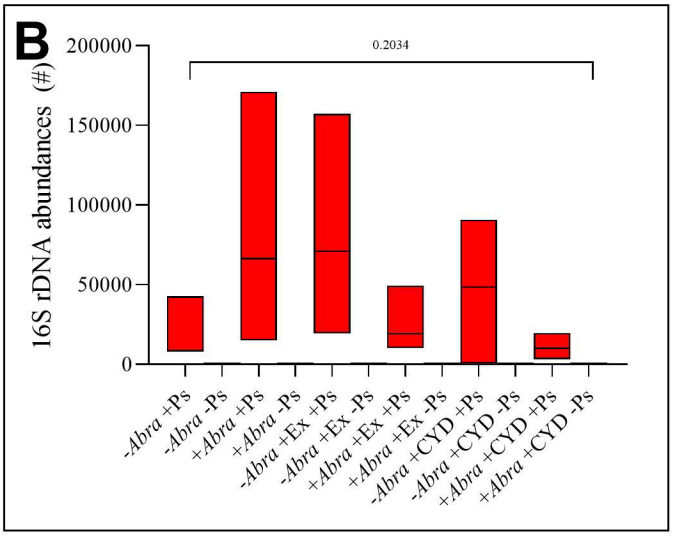
B
16S rDNA abundances (#)
0.2034
-Abra +Ps
-Abra -Ps
+Abra +Ps
+Abra -Ps
-Abra +Ex +Ps
-Abra +Ex -Ps
+Abra +Ex +Ps
+Abra +Ex -Ps
-Abra +CYD +Ps
-Abra +CYD -Ps
+Abra +CYD +Ps
+Abra +CYD -Ps

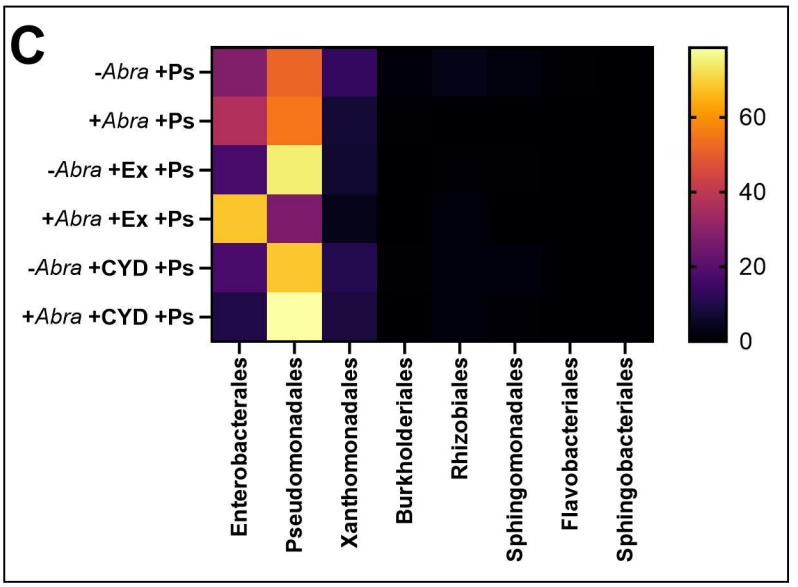
C
-Abra +Ps
+Abra +Ps
-Abra +Ex +Ps
+Abra +Ex +Ps
-Abra +CYD +Ps
+Abra +CYD +Ps
Enterobacterales
Pseudomonadales
Xanthomonadales
Burkholderiales
Rhizobiales
Sphingomonadales
Flavobacteriales
Sphingobacteriales

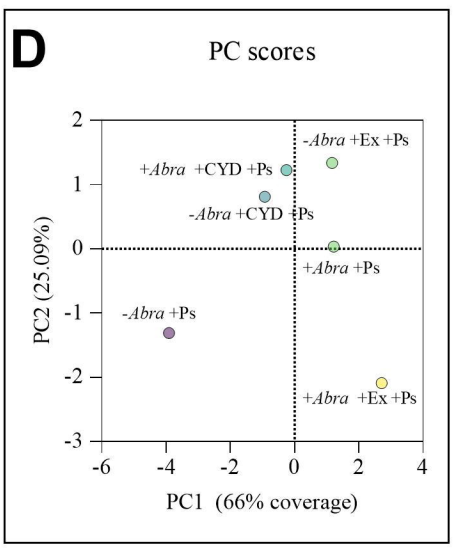
D
PC scores
-Abra +Ex +Ps
+Abra +CYD +Ps
-Abra +CYD +Ps
+Abra +Ps
-Abra +Ps
+Abra +Ex +Ps
PC2 (25.09%)
PC1 (66% coverage)

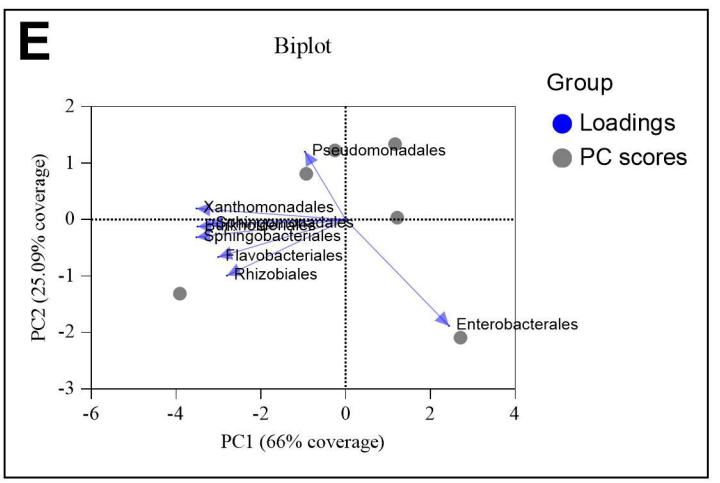
E
Biplot
Group
Loadings
PC scores
Pseudomonadales
Xanthomonadales
Sphingobacteriales
Flavobacteriales
Rhizobiales
Enterobacterales
PC2 (25.09% coverage)
PC1 (66% coverage)

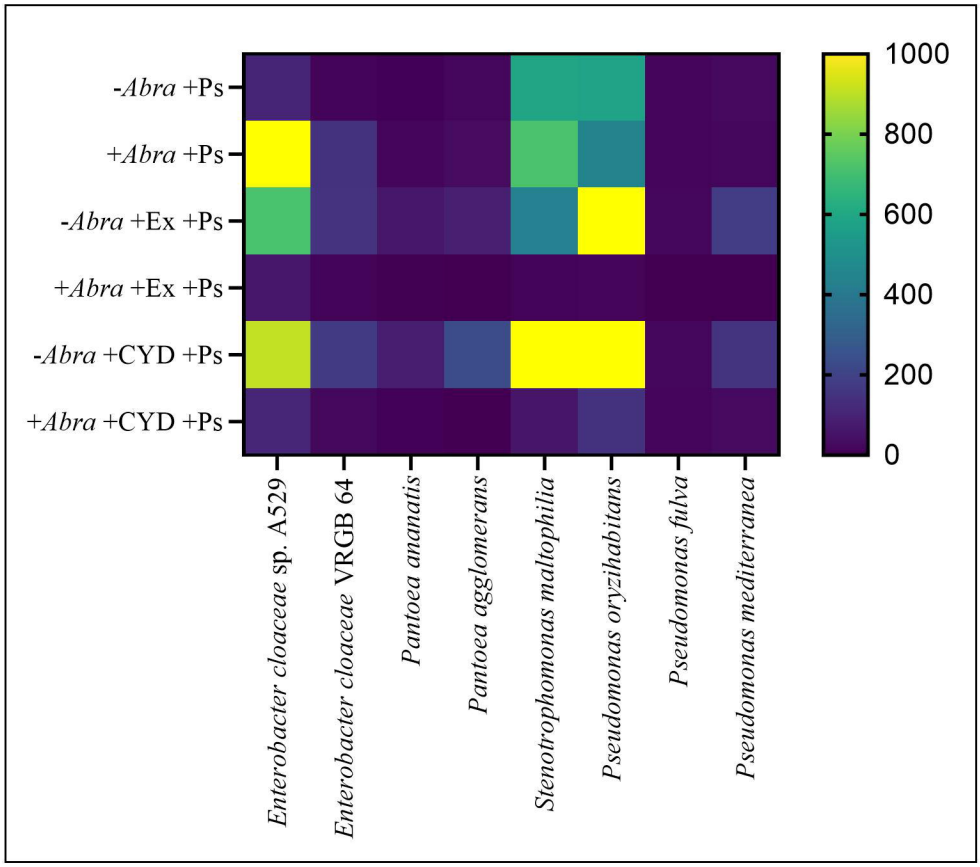
-Abra +Ps
+Abra +Ps
-Abra +Ex +Ps
+Abra +Ex +Ps
-Abra +CYD +Ps
+Abra +CYD +Ps
Enterobacter cloaceae sp. A529
Enterobacter cloaceae VRGB 64
Pantoea ananatis
Pantoea agglomerans
Stenotrophomonas maltophilia
Pseudomonas oryzihabitans
Pseudomonas fulva
Pseudomonas mediterranea
1000
800
600
400
200
0

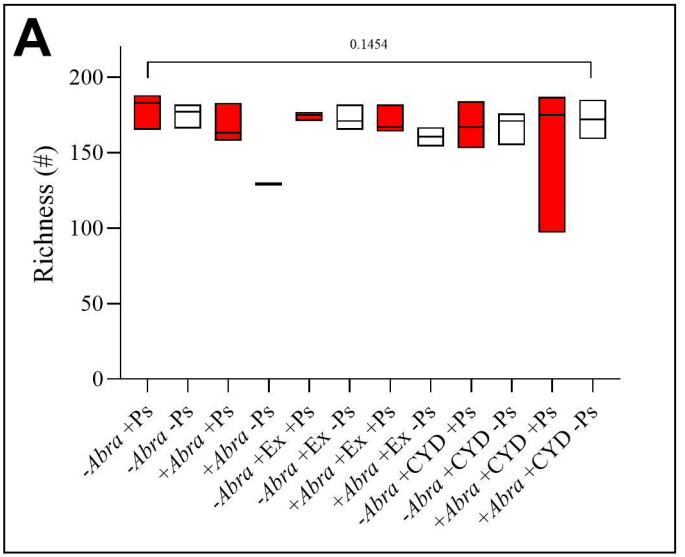
A
0.1454
Richness (#)
200
150
100
50
0
-Abra +Ps
-Abra -Ps
+Abra +Ps
+Abra -Ps
-Abra +Ex +Ps
-Abra +Ex -Ps
+Abra +Ex +Ps
+Abra +Ex -Ps
-Abra +CYD +Ps
-Abra +CYD -Ps
+Abra +CYD +Ps
+Abra +CYD -Ps

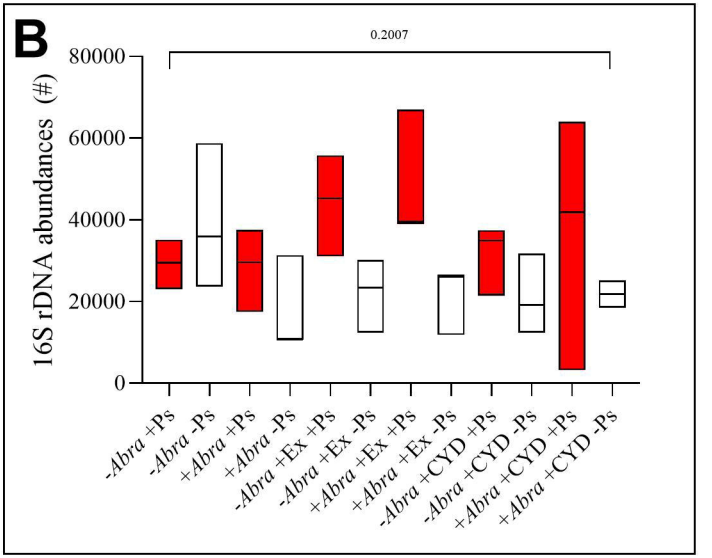
B
0.2007
16S rDNA abundances (#)
80000
60000
40000
20000
0
-Abra +Ps
-Abra -Ps
+Abra +Ps
+Abra -Ps
-Abra +Ex +Ps
-Abra +Ex -Ps
+Abra +Ex +Ps
+Abra +Ex -Ps
-Abra +CYD +Ps
-Abra +CYD -Ps
+Abra +CYD +Ps
+Abra +CYD -Ps

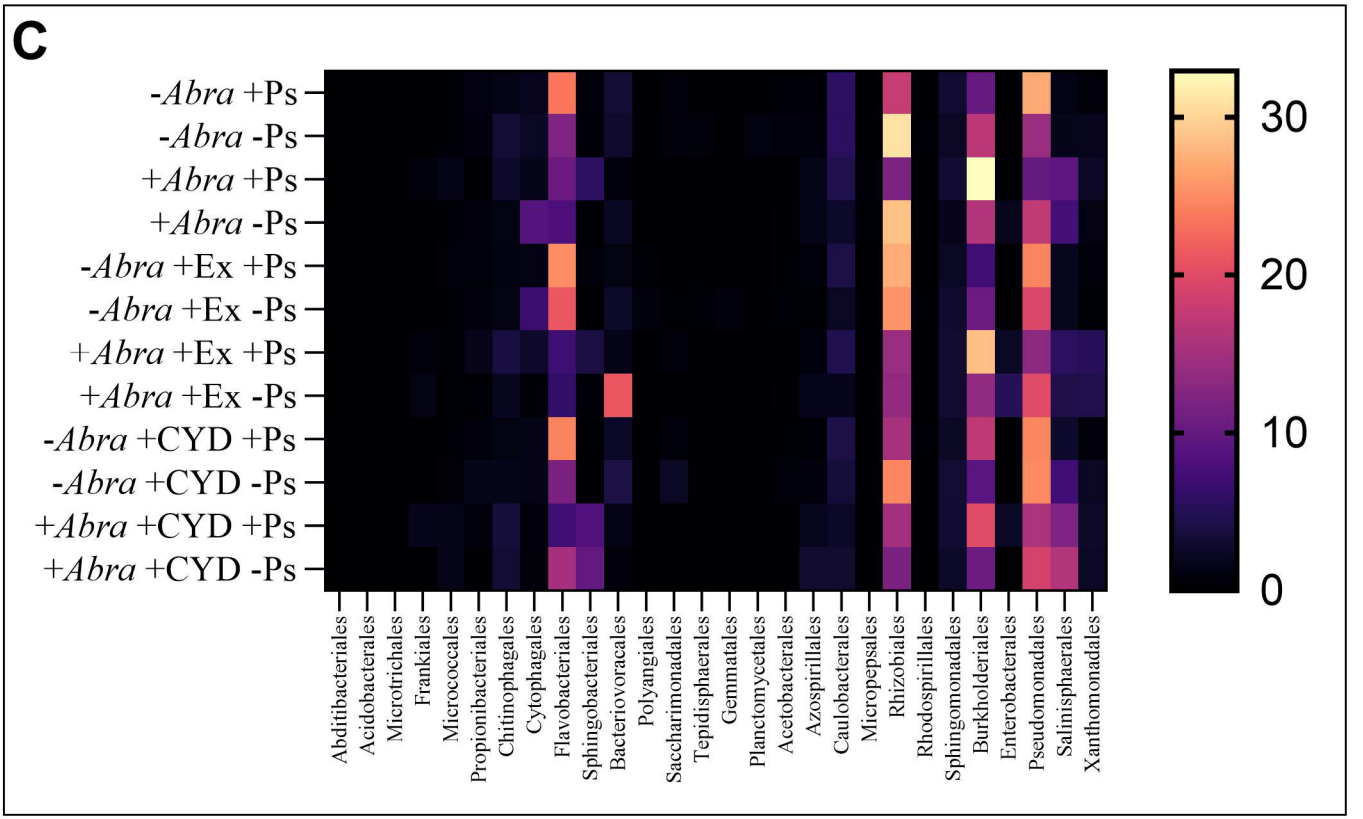
C
-Abra +Ps
-Abra -Ps
+Abra +Ps
+Abra -Ps
-Abra +Ex +Ps
-Abra +Ex -Ps
+Abra +Ex +Ps
+Abra +Ex -Ps
-Abra +CYD +Ps
-Abra +CYD -Ps
+Abra +CYD +Ps
+Abra +CYD -Ps
Abditibacteriales
Acidobacterales
Microtrichales
Frankiales
Micrococcales
Propionibacteriales
Chitinophagales
Cytophagales
Flavobacteriales
Sphingobacteriales
Bacteriovoracales
Polyangiales
Saccharimonadales
Tepidisphaerales
Gemmatales
Planctomycetales
Acetobacterales
Azospirillales
Caulobacterales
Micropepsales
Rhizobiales
Rhodospirillales
Sphingomonadales
Burkholderiales
Enterobacterales
Pseudomonadales
Salinisphaerales
Xanthomonadales
30
20
10
0

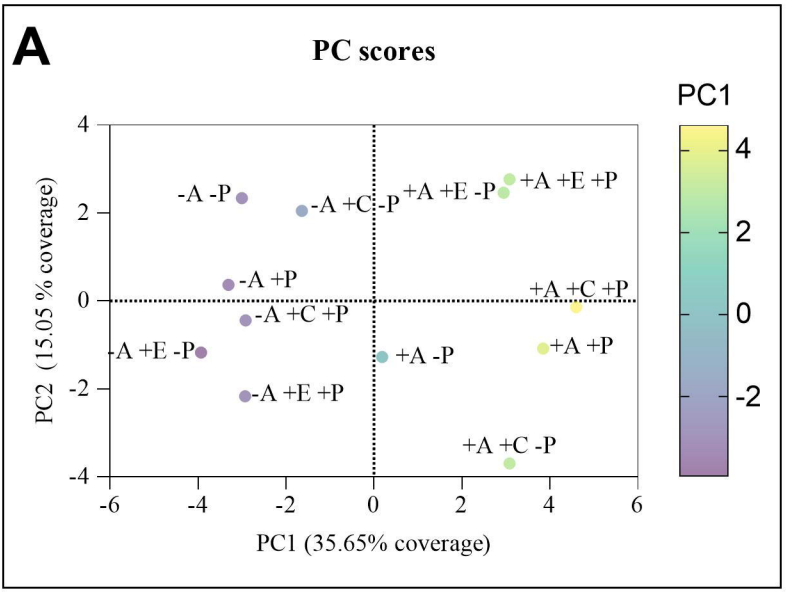
A
PC scores
PC1
4
2
0
-2
-A -P
-A +C -P
+A +E -P
+A +E +P
-A +P
+A +C +P
-A +C +P
-A +E -P
+A -P
+A +P
-A +E +P
+A +C -P
PC2 (15.05 % coverage)
PC1 (35.65% coverage)
-6
-4
-2
0
2
4
6

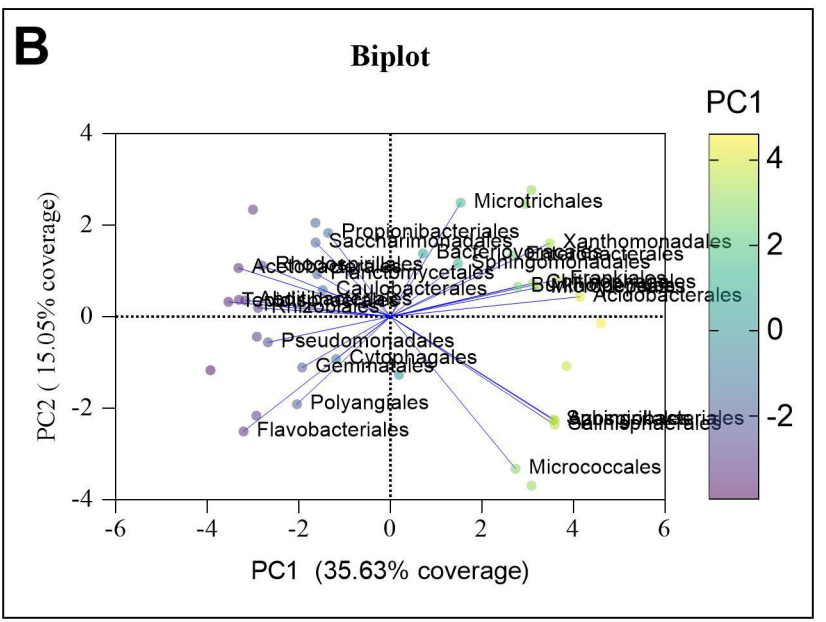
B
Biplot
PC1
4
2
0
-2
Microtrichales
Propionibacteriales
Saccharimonadales
Xanthomonadales
Caulobacterales
Acidobacterales
Pseudomonadales
Cytophagales
Gemmatales
Polyangiales
Flavobacteriales
Micrococcales
PC2 (15.05% coverage)
PC1 (35.63% coverage)
-6
-4
-2
0
2
4
6